From the Department of Molecular Medicine and Surgery
Integrative Physiology,
Karolinska Institutet, Stockholm, Sweden

INSULIN SIGNALLING AND TBC1D1 IN SKELETAL MUSCLE METABOLISM

Ferenc L. M. Szekeres

Stockholm 2011

All previously published papers were reproduced with permission from the publisher.
Cover picture; Ferenc L. M. Szekeres. Shows electroporated muscle, cross section of electroporated muscle and *in vivo* excitation of electroporated *tibialis anterior* muscle.

Published by Karolinska Institutet. Printed by Karolinska University Press
Box 200, SE-17177 Stockholm, Sweden

ISBN 978-91-7457-579-8

To my family

ABSTRACT

Type 2 diabetes mellitus (T2DM) has taken the form of a pandemic disease globally as people adopt a more western lifestyle. High circulating glucose levels indicates that an individual is in the risk zone for developing T2DM. One of the hallmarks for T2DM is insulin resistance in skeletal muscle. Skeletal muscle is the primary target for insulin-stimulated glucose uptake. Thus, it is of clinical importance to understand of how the key hormone, insulin, affects the sensitivity of the tissues to maintain the rate of glucose uptake, and also how glucose uptake could be altered on a cellular level through metabolic switches. The aim for thesis is to investigate whether functional insulin signalling, and hence glucose uptake, occurs in incubated skeletal muscle specimens. Another aim of this thesis is to understand how the molecular switches TBC1D1 and NT5C1A are involved in the regulation of glucose uptake in skeletal muscle.

In paper I, the canonical insulin signalling cascade is investigated in homogenates and cross-sections of skeletal muscle. Muscle specimens were incubated *in vitro,* which is a commonly used experimental technique, to measure glucose uptake and utilisation in skeletal muscle. We show that the canonical pathway of insulin signalling is activated throughout the muscle specimen due to insulin diffusion. We also validate the preparation for the study of insulin signalling. We provide evidence that the experimental approach is valid to assess insulin signalling.

In paper II the effect of silencing the NT5C1A enzyme in skeletal muscle and NT5C2 in cultured myotubes and intact muscle was investigated. We hypothesised that AMPK could be increased if less AMP was hydrolysed as a result of a reduction in the expression of the NT5-enzyme. We demonstrate that in myotubes grown from human biopsies, as well as in mouse *tibialis anterior* muscle, NT5C silencing increases phosphorylation of AMPK and ACC through changes in the AMP:ATP ratio to thereby increase glucose uptake and lipid oxidation. This means that there is alternative approach to activate AMPK and increase glucose uptake, rather than exercise or chemical stimulation, which is a common way to activate metabolism.

In paper III we investigate the role of TBC1D1 in insulin signalling and metabolism. We provide evidence that the TBC1D1-deficient congenic B6.SJL-*Nob1.10* (*SJL/SJL*) mice have enhanced suppression of hepatic glucose production during the euglycemic-hyperinsulinemic clamp. Moreover, glucose uptake in *extensor digitorum longus* (EDL) and *tibialis anterior* muscle was increased during an insulin-stimulated 2-deoxyglucose clamp. Conversely, *in vitro* glucose uptake in response to insulin, contraction or AICAR was impaired in EDL muscle, but not in *soleus* muscle from the *SJL/SJL* mouse. These data provide evidence that TBC1D1 is a regulator of glucose transport and metabolism in skeletal muscle.

In conclusion, insulin signalling is functional in incubated skeletal muscle specimens. Moreover, the molecular switches TBC1D1 and NT5C1A have high impact on glucose uptake in skeletal muscle, which is of great importance for the investigation and understanding of T2DM.

LIST OF PUBLICATIONS

I. Peter Sogaard, **Ferenc Szekeres**, Pablo Garcia-Roves, Dennis Larsson, Alexander V. Chibalin and Juleen R. Zierath. spatial Insulin signalling in isolated skeletal muscle preparations. *Journal of Cellular Biochemistry*. 109(5):943-949, 2010.

II. Sameer S. Kulkarni, Håkan K.R. Karlsson, **Ferenc Szekeres**, Alexander V. Chibalin, Anna Krook, Juleen R. Zierath. Suppression of 5'Nucleotidase enzymes promotes AMPK phosphorylation and metabolism in human and mouse skeletal muscle. *The Journal of Biological Chemistry*. 286(40):34567-34574, 2011.

III. **Ferenc Szekeres**, Alexandra Chadt, Atul S Deshmukh , Robby Z Tom, Alexander V Chibalin, Marie Björnholm, Hadi Al-Hasani, Juleen R Zierath. The Rab-GTPase activating protein TBC1D1 regulates skeletal muscle glucose and lipid metabolism. *Manuscript under review, 2011.*

LIST OF PUBLICATIONS NOT INCLUDED IN THIS THESIS

I. Peter Sogaard, **Ferenc Szekeres**, Maria Holmström, Dennis Larsson, Mikael Harlén, Pablo Garcia-Rove s and Alexander V. Chibalin. Effects on fibre type and diffusion distance on mouse skeletal muscle glycogen content in vitro. *Journal of Cellular Biochemistry*. 107(6):1189-1197, 2009.

II. Peter Sogaard, Mikael Harlén, Yun Chau Long, **Ferenc Szekeres**, Brian R. Barnes, Alexander V. Chibalin and Juleen R. Zierath. Validation of in vitro incubation of extensor digitorum longus muscle from mice. *Journal of Biological Systems*. 18(3):687-707, 2010.

III. Anna Rune, Firoozeh Salehzadeh, **Ferenc Szekeres**, Inger Kühn, Megan E. Osler, Lubna Al-Khalili. Evidence against a sexual dimorphism in glucose and fatty acid metabolism in skeletal muscle cultures from age-matched men and post-menopausal woman. *Acta Physiologica*. 197(3):207-215, 2009.

IV. Isabel Huang-Doran, Louise S. Bicknell, Francis M. Finucane, Nuno Rocha, Keith M. Porter, Y.C. Loraine Tung, **Ferenc Szekeres**, Anna Krook, John J. Nolan, Mark O'Driscoll, Michael Bober, Stephen O'Rahilly, Andrew P. Jackson, and Robert K. Semple. Genetic defects in human pericentrin are associated with severe insulin resistance and diabetes. *Diabetes*. 60(3):925-935, 2011.

CONTENTS

LIST OF ABBREVIATIONS

ACC	Acetyl-CoA carboxylase
ADP	Adenosine diphosphate
AICAR	5-aminoimidazole-4-carboxamide-1-β-$_D$-ribofluranotide
AMP	Adenosine monophosphate
AMPK	Adenosine triphosphate activated protein kinase
ATP	Adenosine triphosphate
CO_2	Carbon dioxide
EDL	*Extensor digitorum longus*
G6P	Glucose-6-phosphate
GDP	Guanosine diphosphate
GLUT	Glucose transporter
GSK3	Glycogen synthase kinase-3
GTP	Guanosine triphosphate
GTR	Glucose turnover rate
IGT	Impaired glucose tolerance
IMP	Inosine monophosphate
IR	Insulin receptor
IRS	Insulin receptor substrate
KHB	Krebs-Henseleit bicarbonate buffer
MHC	Myosine heavy chain
NGT	Normal glucose tolerant
NT5s	5'-Nucleotidases
OGTT	Oral glucose tolerance test
PBS	Phosphate buffered saline
PI3-K	Phosphatidylinositol 3 kinase
shRNA	Small hairpin ribonucleic acid
siRNA	Small interfering ribonucleic acid
T2DM	Type 2 diabetes mellitus
WHO	Word health organization
2-DOG	2-deoxyglucose euglycemic hyperinsulinemic clamp

1 INTRODUCTION

The nutrients for most living organisms can be divided into three major groups, fat, carbohydrates and proteins. Humans tend to eat various sources of nutrients and have done so in a historical perspective, with some nutrition sources being rare and some abundant. What is rare and what is abundant has changed over the last few centuries, and in the western world in particular, now all nutrients are abundant. In an evolutionary perspective, humans have tended to prefer rare nutrients, i.e. carbohydrates, if they had the opportunity. Humans still display this same behaviour, with the difference that there is an oversupply of the historically rare carbohydrates (Cordain *et al.*, 2000). After a carbohydrate rich meal, blood glucose levels rise quickly and there is a need for levels to be normalized. This normalisation is mediated by the hormone insulin (Banting *et al.*, 1922). Skeletal muscle is the major site for clearing blood glucose in response to insulin, and accounts for 75% of the glucose disposal (Baron et al., 1988; Cline et al., 1999). The main glucose transporter in skeletal muscle is the glucose transporter 4 (GLUT4) (Cushman & Wardzala, 1980; Fukumoto et al., 1989), which under basal conditions is located in the cytoplasm. GLUT4 translocates to the plasma membrane to facilitate glucose transport in response to insulin or contraction (Birnbaum, 1989). Type 2 diabetes mellitus (T2DM) is characterized by defects in skeletal muscle glucose uptake (Alberti & Zimmet, 1998). The underlying fault can be regulatory, like a defective signalling pathway, or it can be a genetic defect with one or several genes that are inactive or over-active, or both. A major contributing factor to the development of insulin resistance in T2DM is lifestyle and food habits, with the simple equation: that what we eat, the body must dispose, either store or use as fuel/energy source (Bjorntorp & Sjostrom, 1978).

1.1 TYPE 2 DIABETES MELLITUS

There is also another form of diabetes called type 1 diabetes mellitus, which is the result of an autoimmune destruction of the pancreatic beta cells, which produce insulin. However, the work in this thesis is focused on T2DM. The criterion for getting the diagnosis of T2DM is a blood glucose value above a specific value. The blood glucose value is usually measured as fasting plasma glucose level in millimol per litre (mmol/l), and a fasting concentration of 6.1 mmol/l glucose or above is considered as pathologic and indicative of T2DM (Alberti & Zimmet, 1998). A two hour blood glucose value after an oral glucose tolerance test (OGTT) that is above 11.1 mmol/l is also a criterion for T2DM according to the International Diabetes Federation (www.idf.org). Individuals with T2DM show a lower whole body glucose utilisation, which is mainly the result of reduced insulin-mediated glucose uptake in skeletal muscle (DeFronzo et al., 1985; DeFronzo, 1988). The golden standard to investigate insulin sensitivity in medical research is the hyperinsulinemic euglycemic clamp, during which skeletal muscles account for 80-90% of glucose disposal under insulin-stimulated conditions (DeFronzo, 1988). Insulin signalling has also been shown to be impaired in T2DM patients at the level of insulin binding to the insulin binding to the insulin receptor (IR) (Caro *et al.*, 1987), but also in the phosphorylation of the IR, which is the consecutive step after insulin had bound (Arner et al., 1987; Krook et al., 2000).

1.2 OBESITY

High levels of circulating free fatty acids and large fat depots seem to contribute to skeletal muscle insulin resistance (Boden & Chen, 1995; Roden et al., 1996; Brechtel et al., 2001). Insulin resistance is one factor that connects obesity to the world-wide increase of T2DM. T2DM is considered as a metabolic disorder, which is primarily characterised by insulin resistance, hyperglycemia and impaired insulin secretion (DeFronzo *et al.*, 1985). A person is considered obese if the body mass index (BMI) is above 30 kg/m^2, and overweight if the BMI is equal to or over 25 kg/m^2. The number of obese people is growing dramatically worldwide and since 1980, the number of obese people has doubled (WHO, 2011). In 2008, 200 million men and 300 million women 20 years or older were obese, and in 2010, almost 43 million children younger than five years of age were overweight (WHO, 2011). The stated main reason for this trend for increased obesity according to the WHO is increased food intake and decreased physical activity.

1.3 HYPERINSULINEMIC EUGLYCEMIC CLAMP

The hyperinsulinemic euglycemic clamp measures the amount of glucose necessary to compensate for the particular amount of intravenously infused insulin, without causing hypoglycemia (Shen et al., 1970; DeFronzo et al., 1979b). In humans, after an overnight fast, insulin is infused through a vein at a constant rate of 5-120 mU m^{-2} min^{-1} and 20% glucose solution is infused (GIR) to "clamp" blood glucose at normal levels, around 5-5.5 mmol/l. Blood glucose levels are checked every 5 minutes. The infused insulin sets a new, higher basal insulin level (hyperinsulinemic), which supresses hepatic glucose production (HGP) and increases glucose disposal in skeletal muscle and adipose tissue. Assuming that HGP is totally supressed by the infused insulin, then GIR is equal to the glucose disposal rate, which in turn is equal to the whole body glucose disposal rate (M) for that particular level of hyperinsulinemia. The infused glucose can be radioactive labelled, [3-^{3}H]glucose, and an infusion of [3-^{3}H]glucose 3 hours before and throughout the clamp makes it possible to measure insulin-stimulated whole body glucose turnover rate and also HGP rate. The insulin-stimulated whole body glucose turnover rate is determined as the ratio of infused [3-^{3}H]glucose (dpm/min) to the specific plasma glucose activity for the last 30 min of the clamp. Basal HGP is calculated by the ratio of basal GIR (dpm/min) to the basal plasma glucose specific activity (dpm/μmol). To calculate insulin-stimulated HGP, the glucose infusion rate is subtracted from the whole body glucose turnover rate. The test takes approximately two hours, where a low insulin infusion rate is useful to assess the liver response and a high insulin infusion rate is used to assess the peripheral insulin response. As mentioned before, this test is mostly used in medical research and not in clinical care, where the oral glucose tolerance test (described below) is used instead (DeFronzo et al., 1979a; Kim, 2009).

1.4 ORAL GLUCOSE TOLERANCE TEST

Impaired glucose tolerance (IGT) is one of the hallmarks for the diagnosis a person with increased risk for developing T2DM. A common test to assess a person's glucose tolerance is called the Oral Glucose Tolerance Test (OGTT). The OGTT measures blood glucose two hours after an oral consumption of 75g glucose. Glucose levels below 7.8 mmol/l are considered as normal glucose tolerant (NGT), glucose values between 7.8 and 11.1 mmol/l are considered as IGT and glucose values above 11.1

mmol/l are considered as T2DM (Figure 1). The fasting glucose values for IGT should be below 7.0 mmol/l, which means that the glucose value is too high to be normal, but too low to be classified as T2DM, according to (www.idf.org).

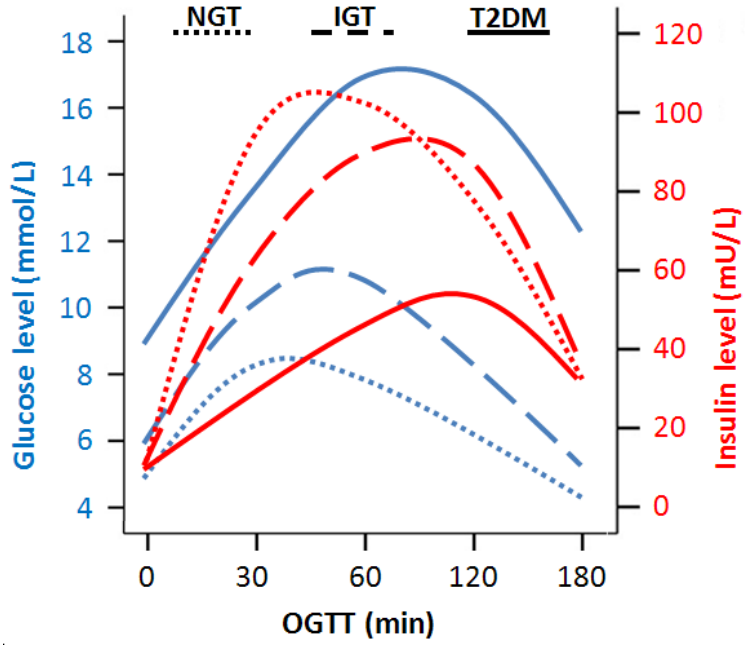

Figure 1: Typical blood glucose and insulin values during OGTT for NGT (Dotted line), IGT (Dashed line) and T2DM (Solid line) patients. Blue lines are glucose levels and red lines are insulin levels.

1.5 INSULIN SENSITIVE TISSUES

Skeletal muscle, adipose tissue and liver are the major organs that respond to insulin. Regulatory mechanisms in these tissues interact mainly with insulin and glucagon. Insulin production and secretion is performed by the pancreatic β-cells in the Langerhans islets in response to high blood glucose (hyperglycaemia), which decreases glucose production (gluconeogenesis) in the liver, reviewed in (Zierath & Wallberg-Henriksson, 1992; Kolaczynski & Caro, 1998; DeFronzo, 2010), and increases glucose disposal in adipose and skeletal muscle. Glucagon is secreted from the pancreatic α-cells in the Langerhans islets in response to low blood glucose levels (hypoglycaemia). Glucagon increases gluconeogenesis in the liver, reviewed in (Thorens, 2008; Edgerton et al., 2009). During hypoglycemia, glucagon is secreted into the circulation reaching the liver, where it increases the gluconeogenesis. Under hyperglycemic conditions, insulin is secreted into the circulation, which decreases gluconeogenesis in the liver and increases glucose uptake in peripheral tissues. In T2DM, insulin secretion is insufficient to lower the blood glucose level. This can be due insufficient amounts of secreted insulin or insulin resistance in peripheral tissues. A first indication of the development of T2DM is often elevated glucose levels and hyperinsulinemia as a compensation for peripheral insulin resistance. However, after a period of time, with increasing blood insulin levels, the pancreatic β-cells fails to secrete the required amount of insulin to maintain normoglycemia, and the insulin level starts to decrease and insulin therapy is required to maintain glucose homeostasis, reviewed in (DeFronzo, 2010).

1.6 SKELETAL MUSCLE

Skeletal muscle is a primary target for insulin action. Mammalian skeletal muscle exhibits a high degree of metabolic flexibility and can shift nutrient source according to

various physiological demands. Calorie restriction both in humans and rodents increases insulin sensitivity in skeletal muscle (Kelley et al., 1993; Cartee & Dean, 1994). Overfeeding (in rodents) induces insulin resistance in skeletal muscle (Wang *et al.*, 2001). Skeletal muscle is composed of individual fibres, which in turn display differences in contractile and metabolic properties. The individual composition of fibres constitutes the metabolic and contractile properties of the muscle. A rough classification of skeletal muscle fibres, depending on their contractile and metabolic properties, is to divide them into: oxidative slow-twitch red fibres (type 1) and glycolytic fast-twitch white fibres (type 2). The glycolytic fibres are less sensitive to insulin compared to the oxidative fibres. The contractile properties are decided by the ratio of myosin heavy chain isoforms (MHC), the most common MHC types are 1, 2A, 2X and 2B (Schiaffino *et al.*, 1989), where muscles composed of predominantly type 1 fibres display slow twitch properties and are highly oxidative, whereas muscles composed mainly of type 2B fibres display fast twitch properties and are mainly composed of glycolytic fibres.

1.6.1 Exercise training

One well known way to improve insulin sensitivity is to exercise (Mikines *et al.*, 1989). Even a single bout of endurance exercise is sufficient to increase insulin sensitivity in skeletal muscle (Richter *et al.*, 1982). Exercise training can transform the phenotype of type 2 muscle fibres from glycolytic to more oxidative characteristics (Schantz & Henriksson, 1983). Exercise training has also proven to have positive impact on T2DM, with increased oxidative capacity, such that fatty acids are used as an energy source and glycogen stores are increased in muscle due to increased insulin sensitivity. Taken together exercise training decreases the risk of T2DM by more than 50% (Rubin et al., 2002; Ilanne-Parikka et al., 2008).

1.6.2 Insulin signalling in skeletal muscle

The insulin molecule binds to the IR on the cell membrane. This results in autophosphorylation of the IR (Van Obberghen *et al.*, 1983) and initiates a signalling cascade downstream of the IR (Kahn et al., 1972; Kahn & White, 1988). The Insulin Receptor Substrate (IRS) is first activated in the cascade, and after that Phosphatidylinositol-3-kinase (PI3-K), Akt and glycogen synthase kinase 3 (GSK3) (Cross et al., 1995; Lee et al., 1995) are activated. The insulin signalling cascade affects glycogenesis (Parker et al., 1983; Roach, 2002; Jensen & Lai, 2009) through phosphorylation of Akt on serine 473 which in turn phosphorylates GSK3 on serine 21 and serine 9, the phosphorylation of GSK3 increases glycogen synthesis by raising the activity of the enzyme glycogen synthase which facilitates the metabolism of glucose into glycogen (Rodriguez & Fliesler, 1988; Pillay & Makgoba, 1991; Smythe & Cohen, 1991). Glycogenesis is inhibited by high levels of glycogen and accelerated by high levels of glucose-6-phosphate (G6P). G6P is the first metabolite during glycolysis. G6P is formed when hexokinase phosphorylates glucose (Roach, 2002; Jensen et al., 2006) Akt also phosphorylates the TBC1 domain family member 1 (TBC1D1) and TBC1D4 and these molecules are considered as the closest signalling proteins to GLUT4, but also the most distant in the insulin signalling cascade controlling GLUT4 translocation (Kane et al., 2002; Roach et al., 2007). Figure 2 shows a schematic overview of insulin signalling in skeletal muscle. Insulin signalling has been thoroughly studied in various cell systems but not so extensively in whole skeletal muscles specimens. Skeletal muscles are multi cellular structures which add an extra dimension in of complexity in the form of fibre bundles grouped into a whole skeletal muscle.

1.6.3 Glucose transport in skeletal muscle

As mentioned above, GLUT4 is the main transporter of glucose in skeletal muscle, and the two major mechanisms by which glucose is transported into the cell is through muscle contraction and/or insulin signalling (Holloszy & Hansen, 1996; Tanti et al., 1997). Muscle contraction depletes the fibres internal stores of ATP and hence, increases the concentration of AMP (Hardie *et al.*, 1999). A low intracellular energy state is indicated with high concentrations of AMP. The depletion of ATP increases glucose transport by translocating GLUT4 to the plasma membrane and glucose diffusion is facilitated. One of the molecular mechanisms involved in this insulin-independent pathway is via AMP-activated protein kinase (AMPK) (Musi *et al.*, 2001). A chemical compound, 5-aminoimidazole-4-carboxamide-1-β-$_D$-ribofluranotide (AICAR), mimics the effect of AMP on AMPK (Merrill *et al.*, 1997). AICAR is metabolized to a monophosphorylated derivative (ZMP) by adenosine kinase (AK), which is an analogue of AMP and activates AMPK by increasing the ZMP/ATP ratio. AICAR is used as a biochemical agent to mimic the activation of AMPK by AMP and it is used to study the role of AMPK in metabolism (Corton *et al.*, 1995).

1.6.4 Glucose transport and TBC1D1

In the basal state, GLUT4 can be tethered and prevented from reaching the plasma membrane by special Rab GTPase activating proteins namely TBC1D1 and TBC1D4. Both TBC1D1 and TBC1D4 contain GAP domains to which specific Rab protein bind. When bound, the glutamine residue in the Rab protein gets aligned with arginine in the TBC domain and this this accelerates the hydrolysis of GTP by stabilizing the protein to protein interaction (Scheffzek et al., 1998; Rak et al., 2000). Rab proteins are small G proteins that are required for vesicle trafficking. The function of G proteins is to work like a molecular switch; if they have bound GTP they are “on” and if they have bound GDP they are “off”. TBC1D1 is active in its unphosphorylated state and thereby tethers GLUT4 molecules by hydrolysing GTP to GDP and hence decreasing the rate of glucose transport into the cell (Figure 2). Mice lacking TBC1D1 through a natural occurring deletion in the gene have reduced GLUT4 protein levels (Chadt *et al.*, 2008). Reduced expression of TBC1D1 in skeletal muscle cells increases both the uptake and oxidation of fatty acids (Chadt *et al.*, 2008). To make a rough distinction of the tissue distribution, one can say that TBC1D1 is the most abundant in type II skeletal muscle fibres, whereas TBC1D4 is most abundant in type I skeletal muscle fibres and white adipose tissue from mouse. Nevertheless, the precise role of TBC1D1 in the regulation of cellular response to insulin or activators of the cellular stress signalling cascade is unknown. Furthermore, the role of TBC1D1 in the regulation of whole body glucose uptake has not been investigated.

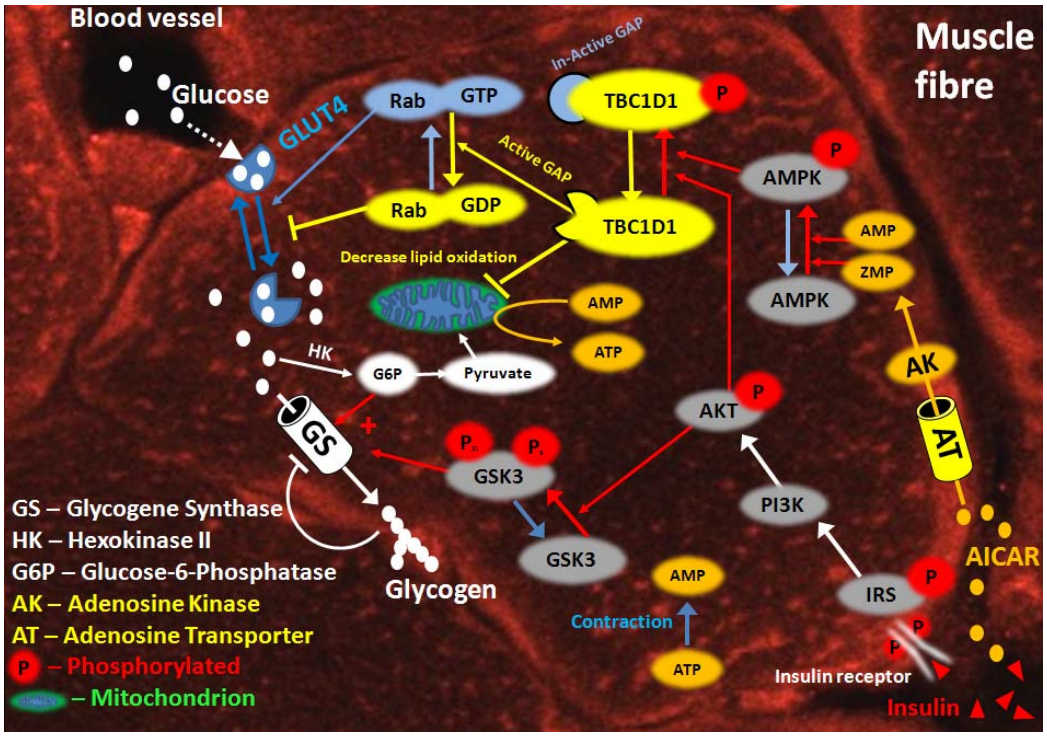

Figure 2: Insulin-dependent and -independent glucose uptake. Insulin stimulation leads to the phosphorylation of Akt, which then inactivates TBC1D1. TBC1D1 can also be phosphorylated by AMPK. When TBC1D1 is phosphorylated, the GAP binding site is unable to bind and hydrolyse GTP to GDP, which in turn makes the Rab-protein active. Hence, GLUT4 translocation is promoted and glucose uptake increases.

1.6.5 Fatty acid metabolism in skeletal muscle

Fatty acid oxidation occurs in the mitochondria by β-oxidation, and the availability of fatty acids is the regulating step for oxidation, reviewed in (Ruderman *et al.*, 1999). The enzyme carnitine palmitoyl transferase 1 determines the rate of fatty acid oxidation by controlling the transfer of long chain fatty acids into the mitochondria (McGarry, 1995). Malonyl-CoA is the substrate, carboxylated from acetyl-CoA, which enters the citric acid cycle. Acetyl-CoA is the product from the break-down of fatty acids in the form Acyl-CoA in the mitochondria. The formation of malonyl-CoA can be prevented by blocking the enzyme acetyl-CoA carboxylase (ACC), which forms malonyl-CoA. AMPK is also involved in the formation of malonyl-CoA. When AMPK is activated it blocks ACC activity by phosphorylation (Winder & Hardie, 1996). AMPK also promotes (Saha *et al.*, 2000) and blocks (Habinowski *et al.*, 2001) decarboxylation of malonyl-CoA by acting on the enzyme malonyl-CoA decarboxylase. Exercise increases fatty acid oxidation in skeletal muscle. Figure 3 provides a schematic picture of fatty acid metabolism in skeletal muscle.

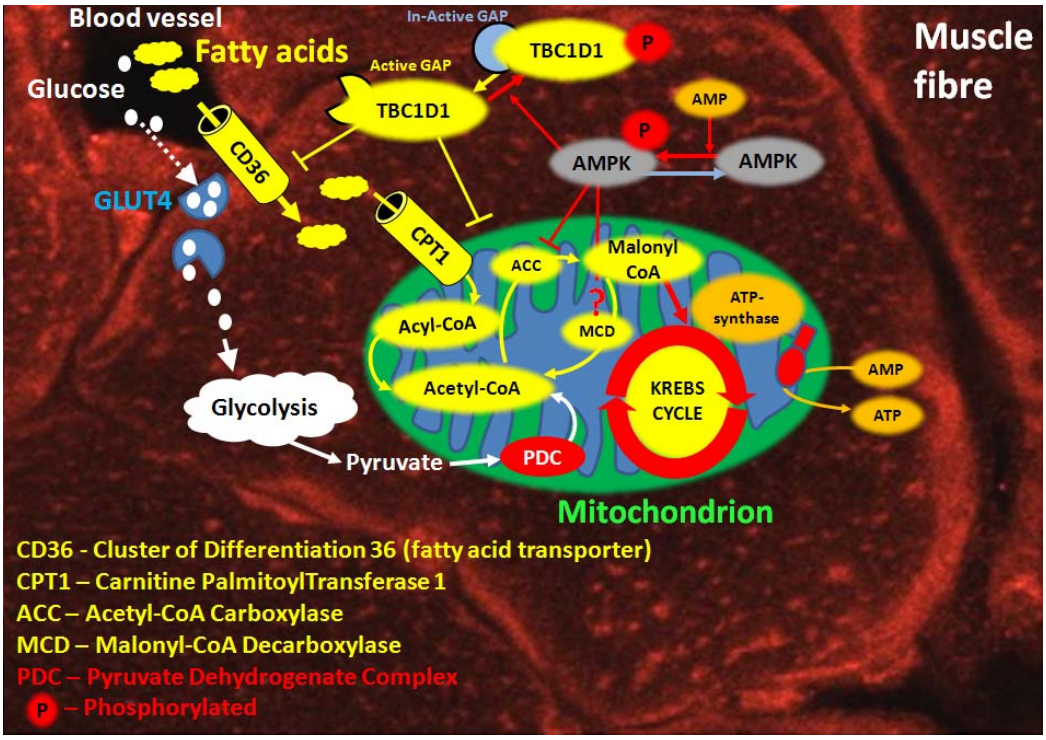

Figure 3: Fatty acid oxidation in skeletal muscle. Phosphorylated AMPK inhibits fatty acid oxidation by phosphorylation of the enzyme ACC. TBC1D1 has a negative impact on the uptake of fatty acids and fatty acid oxidation. AMPK has a dubious role regarding the enzyme MCD, both as activator and suppressor; this is reflected by the question mark on the line between AMPK and MCD.

1.7 5'-NUCLEOTIDASES

5'-Nucleotidases (NT5s) are a family of enzymes that catalyse the hydrolysis of non-cyclic nucleotide monophosphates to nucleosides and inorganic phosphate. The role of intracellular NT5s is to maintain a balance in DNA and RNA synthesis by regulating the intracellular pool of nucleotides **(**Figure 4). NT5C1 prefers AMP as a substrate and is highly expressed in heart and skeletal muscle (Gibson & Drummond, 1972). NT5C2 prefers Guanine Monophosphate (GMP) and Inosine Monophosphate (IMP) as substrates, but has an overlapping affinity towards AMP (Banditelli *et al.*, 1996). The NT5-enzymes play a central role in maintaining the intracellular levels of ADP and ATP and can therefore indirectly regulate the AMPK activity. NT5-enzymes may regulate the catabolic pathways and production of ATP via AMPK (Spychala et al., 1988; Hanisch et al., 2006; Careddu et al., 2008).

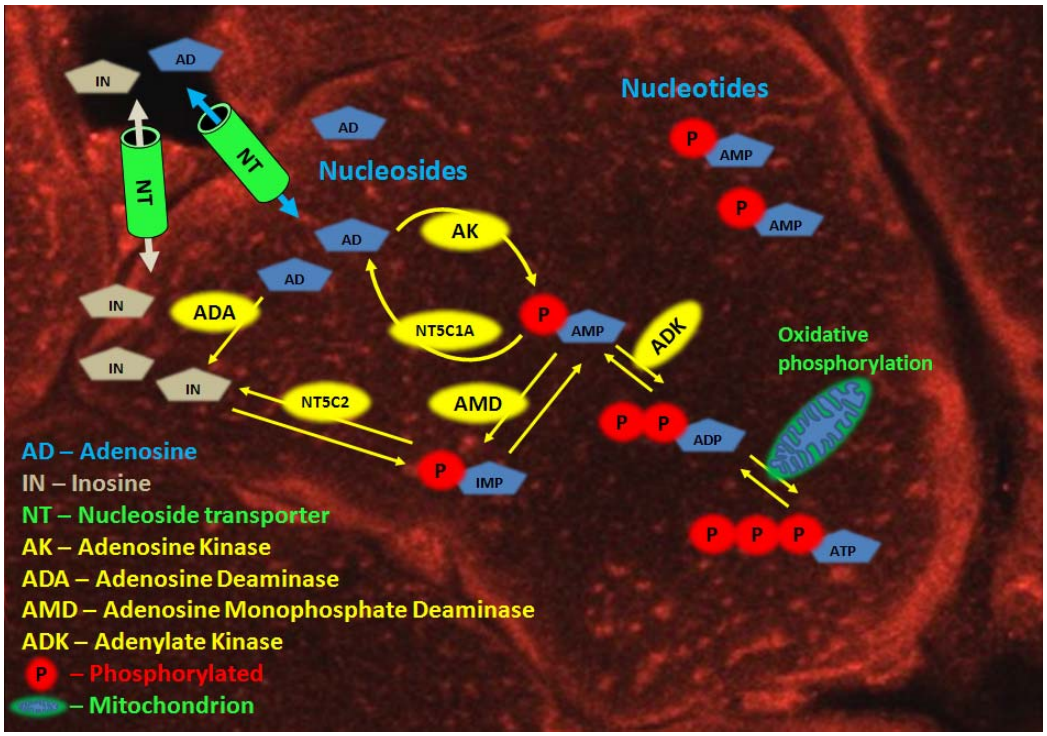

Figure 4: Nucleotidases in skeletal muscle. NT5C1A dephosphorylates AMP to adenosine which then can be transported out of cell. NT5C2 dephosphorylates IMP to Inosine which then can be transported out of the cell. This will negatively influence the intracellular available pool of nucleotides (e.g. AMP), leading to less ADP and ATP.

Nucleotides do not appear to be transported over the plasma membrane. However, after the NT5-enzyme has dephosphorylated the nucleotide to a nucleoside, it can be transported out of the cell by facilitated diffusion (Gazziola et al., 2001; Hunsucker et al., 2005).

Given the central role of NT5-enzymes in controlling and maintaining the intracellular levels of ADP and ATP they may provide an alternative pathway to indirectly regulate the AMPK activity and hence control glucose and lipid metabolism. Thus, gene silencing of NT5-enzymes to increase the intracellular availability of AMP may increase AMPK activity and metabolism. However, this approach has yet to be tested.

2 AIM OF THE THESIS

The hypothesis for this thesis is that insulin signalling is triggered throughout the muscle specimen during *in vitro* incubation. TBC1D1 and NT5C1A are molecular switches affecting glucose uptake in skeletal muscle. To this end *in vitro* and *in vivo* metabolic experiments in mouse skeletal muscle, and cultured human muscle have been performed. Specific aims are outlined below.

- To determine if the insulin signalling cascade is triggered due to diffused insulin in *in vitro* incubation of muscle specimens.
  - Specifically, we determined whether insulin is able to diffuse across the entire muscle specimen in sufficient amounts to activate signalling cascades to promote glucose uptake and glycogenesis within isolated mouse skeletal muscle.

- To investigate the role of 5´-nucleotidases in skeletal muscle metabolism.
  - We hypothesized that gene silencing of NT5 enzymes to increase the intracellular availability of AMP would increase AMPK activity and metabolism in order to elucidate the role of cytosolic NT5 in metabolic responses linked to the development of insulin resistance in obesity and type 2 diabetes mellitus.

- To validate the role of TBC1D1 in skeletal muscle metabolism.
  - We determined whether TBC1D1 is involved in insulin, as well as energy-sensing signals controlling skeletal muscle and whole body metabolism.

3 METHODS

3.1 ANIMALS

Mice were maintained in light and temperature controlled environment and had free access to water and standard rodent chow. Mice used for the *in vitro* experiments were anaesthetized with Avertin (2,2,2)-Tribromo ethanol 99% (0.5 µl per gram of body weight, intraperitoneal), and thereafter *Soleus* and EDL muscles were rapidly dissected and kept in a oxygenated (95% O_2, 5% CO_2) Krebs-Henseleit bicarbonate buffer (KHB) at 30°C. Mice studied for the *in vivo* experiments (clamp surgery and electroporation) were anaesthetized with Isoflurane (~2% of breathing air), and a pain killer was administered (Rimadyl, subcutaneously, 5 mg/kg bodyweight) directly after the surgical procedure and the following day. All experimental procedures were approved by the regional Ethical Committee in Stockholm.

3.1.1 Wild type animals

The C57Bl/6J mouse was used as a wild type (control) animal in the *in vitro* muscle incubations, unless otherwise stated.

3.1.2 TBC1D1 animals

The TBC1D1 animals have a 7 base pair deletion in the TBC1D1 gene in exon 18. The deletion gives a TBC1D1-deficient congenic B6.SJL-*Nob1.10* (*SJL/SJL*) mouse. The transgenic TBC1D1 mice and litter mates homozygous for the wild type exon 18 (*B6/B6*) were studied (Chadt *et al.*, 2008).

3.2 METABOLIC MEASUREMENTS AFTER *IN VITRO* INCUBATION

The incubation media used for the *in vitro* study was composed of a Krebs-Henseleit bicarbonate buffer (KHB) supplemented as specified in the Papers for each particular experiment. The basal incubation buffer contained 5 mM glucose, 15 mM mannitol, 5 mM HEPES and 0.1% bovine serum albumin (BSA). Muscles were incubated at 30°C oxygenated (95% O_2, 5% CO_2) in a shaking water bath. The animals were fasted 4 hours before each experiment.

3.2.1 Insulin and AICAR stimulated glucose transport

The assessment of glucose transport in *in-vitro* incubated mouse skeletal muscle consists of four incubation steps:
Recovery → Pre-incubation → Rinse → Hot incubation, below follows a more detailed description of each step.
Recovery continued for 30 min in basal media for the muscles to recover from surgery.
Pre-incubation was performed in either basal, insulin (120 nM) or AICAR (2 mM) complemented KHB.
Rinse continuous for 10 min in which the muscle was incubated in a glucose-free buffer containing 20 mM mannitol.
Hot incubation was performed with radioactive labelled tracer for 30 min, in the presence of either AICAR (2 mM) or insulin (120 nM) with KHB supplemented with 1 mM 2-deoxy-[1,2,^{3}H]glucose (2.5 µCi/ml) and 19 mM [^{14}C]mannitol. The last step was included to wash the muscles in ice-cold KHB. The muscles were then blotted on filter

paper, and freeze-clamped with a precooled tong in liquid nitrogen. Thereafter the muscles were stored in -80°C until analysis. Glucose transport was measured by scintillation counting of the intracellular accumulation of 2-deoxy-[1,2,^{3}H]glucose and expressed as nmol glucose per mg of protein per 30 min.

3.2.2 Contraction-stimulated glucose transport

For the determination of contraction-induced glucose uptake, the same protocol was used as described for insulin- and AICAR-stimulated glucose transport, with some minor modifications. The pre-incubation step was exchanged for a 10 min contraction stimulus. The isolated muscles were placed in an incubation chamber with continuously oxygenated basal KHB. The distal tendons were fixed at the bottom of the chamber and proximal tendons were connected to a force transducer (Harvard Apparatus) and the resting tension was set to 0.5 g. The muscles were stimulated at frequency of 100 Hz, 0.2 ms pulse length with 20 V, every 2 sec for 10 min. Figure 5 shows the contraction apparatus.

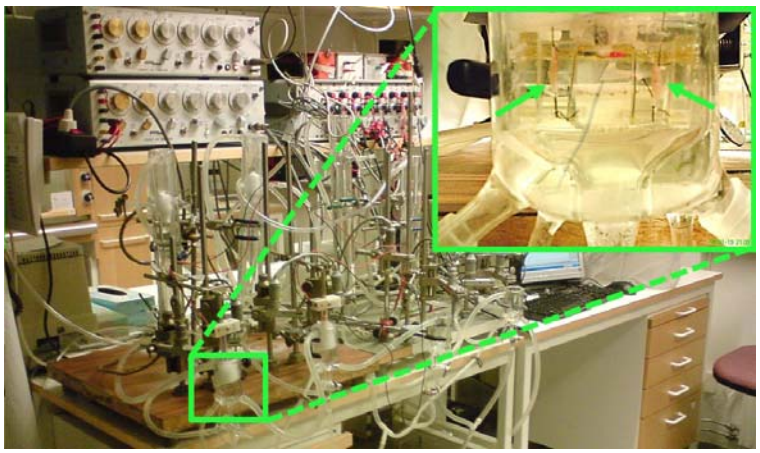

Figure 5: The contraction apparatus, along with the Harvard Apparatus force transducer, the green arrows on the close-up shows a muscle specimen during the contraction procedure placed in a chamber filled with KHB.

3.2.3 Glucose incorporation into glycogen and glucose oxidation

Glucose incorporation into glycogen and glucose oxidation was assessed in *Soleus* and EDL muscles. Muscles were incubated at 30°C for 60 min in 2 ml of KHB supplemented with 5 mM [U-^{14}C]glucose (0.3 µCi/ml), in a flask sealed with a rubber stopper. Each flask contained a centre-well which collected the CO_2 released into the media from the muscle. Immediately after incubation, 200 µl of protosol was injected into the centre-well via a syringe through the rubber cap, and the flasks were placed in ice-cold water bath for 3 min. Thereafter, the flasks were quickly opened and the muscle was removed and placed on ice-cold filter paper and trimmed of tendons, weighed and freeze clamped. After the flasks were resealed, 15% PCA was injected via a syringe into the media, followed by continuous incubation for 60 min and the released [U-^{14}C]CO_2 was collected into the centre-well containing protosol. After the incubation, 150 µl of the protosol in the centre-well was pipetted into 20 ml scintillation vials. This step was included to ensure that the same volume was used for scintillation counting of all samples, rather than taking the whole centre-well and placing it in the scintillation vial. Using the latter approach, it could be possible to get different volumes and also contamination from the media on the outside of the centre well. Thereafter, 10 ml of scintillation fluid and 200 µl of 5N HCL was added to all vials, after which they were mixed and stored at 4°Cfor 60 min before counting in the β-counter. The incubated muscles were dissolved with 0.5 ml of 1M NaOH at 70°C for 30 min. Thereafter, 0.5

ml of 20% TCA was added for deproteinization, the samples were vortexed and subjected to centrifugation at 3,500 g at 10°C for 15 min. The supernatants were pipetted into new tubes, to which 200 µl of glycogen solution (100 mg glycogen in 5 ml of dH_2O) and 2 ml of ethanol was added. This glycogen serves as a carrier for the radioactive glycogen. The tubes were placed at -20°C overnight, after which the tubes were subjected to centrifugation for 15 min at 2,000 g. Thereafter, the supernatant was discarded and the pellet was dissolved in 0.7 ml of dH_2O. Aliquots of 500 µl were measured in scintillation vials with the same procedure as for the released CO_2.

3.3 METABOLIC MEASUREMENTS *IN VIVO*

3.3.1 Euglycemic Hyperinsulinemic clamp

The mice for clamp experiments underwent surgery 7 days before the actual experiment. During the surgery, a catheter was placed in the left jugular vein towards the heart. The catheter was drawn up on neck of the mouse and then connected to a pump, which was used for the insulin and glucose infusion. Animals were fasted 4 hours before the actual clamp experiment.

3.3.1.1 Euglycemic Hyperinsulinemic clamp

During the euglycemic hyperinsulinemic clamp, glucose turnover rate (GTR) and hepatic glucose production (HGP) were determined, approximately 60 min after tracer infusion. GTR was measured in the basal state, with a constant infusion of [3-^{3}H] glucose (0.09 µCi/min). The bolus injection was 2.5 µCi. The priming dose of insulin (25 mU/kg) was administered before the constant rate of insulin infusion (2.5 mU/kg/min). Steady state was reached approximately 60 min after administering a bolus of insulin. During steady state, blood samples were obtained and used to measure HPG (the average glucose infusion rate subtracted from the glucose utilisation) and whole body glucose utilisation. Blood samples were taken at the basal and insulin-stimulated condition to measure circulating insulin levels.

3.3.1.2 2-Deoxyglucose Euglycemic Hyperinsulinemic clamp

The 2-deoxyglucose euglycemic hyperinsulinemic (2-DOG) clamp was performed to access tissue-specific glucose uptake. A bolus of insulin (40 mU) was administered at the start of the clamp and the insulin infusion rate was maintained at 75 mU/min/kg. Blood glucose values were monitored at 5 min interval. The glucose infusion was increased until the target basal glucose value was reached and remained stable. At this stage the tracer was injected (3 µCi) and blood samples were taken at 0, 3, 6, 10, 15, 20, 30, 40 and 60 min. At this point the animals were euthanized with an overdose of sodium pentobarbital and the tissues were collected. The tissues were lysed in 0.5 ml NaOH for 60 min at 60°C and neutralized with 0.5 ml of HCL. The homogenates was divided and into two samples; 0.2 ml for analysis with $Ba(OH)^2$ and $ZnSO_4$ and 0.2 ml taken for analysis with 6% PCA. The samples were mixed with a vortex and centrifuged. Thereafter, 0.8 ml of the supernatant was pipetted into a scintillation vial containing 10 ml of scintillation fluid. The samples were subjected to scintillation counting. The results were calculated as [$Ba(OH)^2$,$ZnSO_4$]-cpm values subtracted from the [PCA]-cpm values.

3.4 ELECTROPORATION

With electroporation, a polar molecule like a plasmid or DNA is introduced into the cell through the membrane by electrical stimulation. The electrical stimulation creates pores in the cell membrane in which foreign DNA can enter, the pores will close by themselves and the DNA are trapped inside the cell where it can use the cells endogenous machinery to produce mRNA and thereby protein (McMahon & Wells, 2004).

3.4.1 Knock down of NT5C1A with electroporation

To reduce expression of NT5C1A, a pool of shRNA plasmids targeted against NT5C1A (SABiociences) was used. The *tibialis anterior*, in 12-14 weeks old C57Bl/6 mice was targeted. Prior to electroporation, the *tibialis anterior* muscle was injected with hyaluronidase to permeabilize the muscle. After a 2 hour incubation, the plasmids were injected and thereafter the leg was electrically stimulated with the ECM 830 square wave electroporation system (BTX, Harvard apparatus, Holliston, MA), using contact gel to ensure good conductivity with the calliper electrodes.

3.4.1.1 Glucose uptake in tibialis anterior muscle after electroporation

Mice were fasted for 4 hours, thereafter a bolus of glucose (3 g/kg) was administered by gavage. An intraperitoneal injection of [^{3}H]-glucose (4.5 µl 3H-2DG per 100 µl of saline per animal, 1 mCi/ml) was administered. 2 hours after injection the *tibialis anterior* was dissected out and frozen in liquid nitrogen. Muscles were homogenised in-ice cold buffer (10% glycerol, 5 mM sodium pyrosulphate, 13.7 mM NaCl, 2.7 mM KCl, 1 mM MgCl2, 20 mM Tris (pH 7.8), 1% Triton X100, 10 mM NaF, 1 mM EDTA, 0.2 mM phenylmethylsulfonyl fluoride, 1 µg/ml aprotinin, 1 µg/ml leupeptin, 0.5 mM sodium vandanate, 1 mM benzamidine, 1 µM microcystin) using a motor driven pestle for 20 seconds. Samples were rotated for 1 hour at 4°C, and then subjected to centrifugation (12,000 g for 10 min at 4°C) after which, 30 µl of the supernatant was subjected to scintillation counting, and the remaining portion of the supernatant was stored at -80°C for western blot analysis.

3.5 IMMUNOHISTOCHEMISTRY

3.5.1 Cryostat sectioning

Frozen muscles were sectioned with a Microm HM 500 M at -23°C to 12 µm thickness and mounted on SuperFrost (Menzel GmbH & Co) microscope slides and air dried for 45 min at room temperature. To ensure that the outer most layer of cells remained intact, the muscle was not submerged in OCT (Tissue-Tek, Sakura Finetek, NL), but rather sectioned "free-standing" on a pre-holed cork plate where one end of the muscle was placed in the hole and surrounded with OCT. Microscope slides were stored at -20°C until analysis.

3.5.2 Immunofluorescence

Microscope slides were thawed for 15 min, after which all subsequent steps were performed at room temperature. The slides were rehydrated with phosphate buffer solution (PBS) containing 0.2% Triton X-100 (PBT) for 20 min, and blocked with PBT containing 1% BSA for 30 min. After this, incubation was performed using an antibody

solution in diluted PBT for 2 hours. Zenon Alexa Flour 555 rabbit IgG labelling reagent was used (Z-25305, Invitrogen, Sweden). Thereafter, the slides were washed 3 times for 15 min in PBT, and once in PBS for 5 min. The samples were fixated with 4% formaldehyde in PBS for 15 min and washed one more time in PBS for 5 min. Mounting was performed with ProLong Gold anti-fade reagent containing DAPI (P36931, Invitrogen, Sweden). The Zenon Alexa Flour 555 rabbit IgG labelling reagent (Fab-fragments) was used to fluorescently mark primary antibodies. The ratio between Fab-fragments and the antibody was 6:1 and the ratio of the dilution in the final working solution with PBT and the antibody solution was 6:1. Antibodies against phosphorylated insulin receptor (pIR-Tyr1146), phospho-Akt (pAkt-Ser473) and phoshpo-glycogen synthase kinase 3 (GSK3α/β-Ser21/Ser9) were used. Imaging was performed with a confocal microscope, inverted Zeiss LSM 510 META (Settings: Plane, multitrack, 12 bit, 1,024_1,024, 1,303.0 mm_1,303.0 mm, Plan-Neufluar 100/0.3, and for the 630x magnifications, Plan-Apochromat 63x/1.4 Oil DIC).

3.5.3 Quantification of immunofluorescence staining

For all images taken, the setting of the microscope and camera were kept equal and background subtraction was not made. For each picture, three standardised regions of 50 x 200 pixels were taken. This procedure was repeated for three muscle slices per specimen. Thus in total, nine regions from each muscle were analysed (Figure 6).

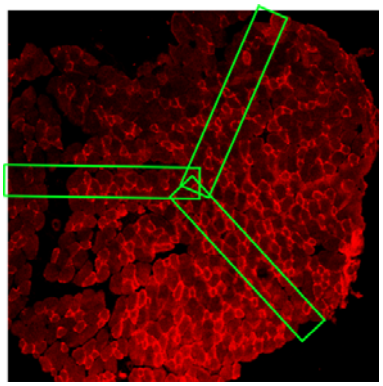

Figure 6: Example of the three regions of 50 x 200 pixels that were used for the analysis. In this figure, an antibody against pIRTyr^{1146} was used to study insulin-stimulated EDL muscle.

All nine regions were pooled together to obtain a robust estimate of the mean intensity. The standardized regions were extracted using MATLAB (MathWorks), and the pictures were rotated in Photoshop before excising the regions, so that an undamaged muscle region was facing the left side of the picture (Figure 7).

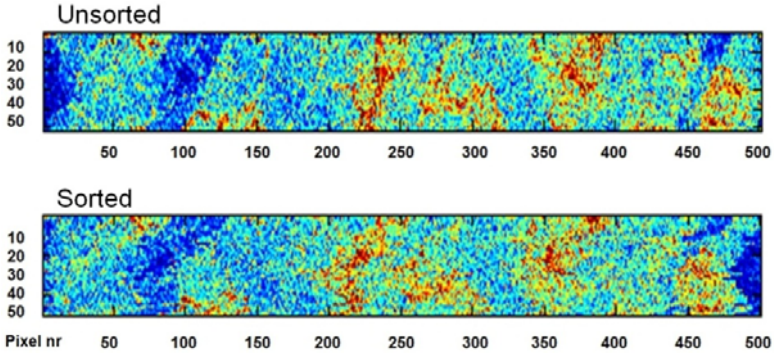

Figure 7: Example of unsorted and sorted regions of 50x500 pixels treated as a matrix of pixel values, divided into 9 groups of 50 pixels each.

The standardised region was treated as a matrix and aligned so that the border of muscle section reflected the first pixel column. The matrix was then divided into 9 groups of 50 pixels, and for each, the group mean was calculated to get a single set of data. Data were normalised against group 1 in the matrix, and against the control of each group to determine whether any difference occurred between the treatments (Figure 7).

3.5.4 Capillary staining

Capillary staining of skeletal muscle was performed with an indoxyl-tetrazolium method for alkaline phosphatase, which reveals the enzyme located in the capillary endothelium (Ziada *et al.*, 1984). *Tibialis anterior*, *Soleus* and EDL were bundled together and sectioned simultaneously. Staining was performed as described earlier (Ziada *et al.*, 1984). Muscle sections were incubated for 1 hour at 37°C, using an incubation medium composed of: nitroblue tetrazolium (Sigma), 30 mg; 5-bromo 4-chloro 3-indolyl phosphate p-toluidine salt (Sigma), 6 mg in 30 ml of a buffer containing 6.9 mM $MgS0_4$ and 27.5 mM $NaB0_2$, pH adjusted to 9.2-9.4 with boric acid. A 5 min post-fixation in sucrose buffered formalin (4% formaldehyde, pH 7.3, 300 mOsmol; 5 min) was performed after rinsing. Thereafter, muscle sections were alcohol dehydrated and mounted. The free-ware program Image-J (http://rsbweb.nih.gov/ij/) was used for analysis. With the Image-j program background was subtracted, threshold adjusted, and the image processed to binary and finally subjected to watershedding. Thereafter, the stained capillaries were counted with the "analyse particle" function. The number of fibres per section was counted manually from the unprocessed picture.

3.6 LUMINEX SYSTEM

The Luminex system used here is the Bio-Plex 200 system from Bio-Rad (Bio-Rad, Richmond, CA). The Bio-Plex 200 system works on the Luminex xMAP 96-well platform format. This technology (theoretically) permits simultaneous detection of up to 100 different analytes in one sample. The Luminex system uses an array of up to a 100 sets of beads with a diameter of 5.6 μm. Each set of beads has an internal colour which gives the bead an identity number from 1-100. The core of the system is the bead with the internal colour which is coated with antibodies of a particular target. The Bio-Plex 200 machine has two lasers, one that confirms the internal colour of the bead and thereby the particular target, and another laser by which the machine quantifies the actual amount of the target bound to the antibodies of the bead. The advantage of the Luminex xMAP technology is the possibility of multiplexing, meaning that the antibody coated beads can be mixed and up to (theoretically) 100 different targets which can be analysed for each and every well of the plate. Usually each kit also comes with a standard curve so that the outcome may be related back to an absolute concentration of the particular target (www.bio-rad.com).

3.6.1 Luminex assay

The Luminex kits used were obtained from Bio-Rad, special ordered in a 3-plex fashion, for pIR, pAkt, and pGSK3, (all these analytes are commercial available). The assay was performed according to the manual for the phosphoprotein kit (www.bio-rad.com).

3.7 CELL CULTURE OF HUMAN SKELETAL MUSCLE

Muscle biopsies were obtained from *rectus abdominis* during abdominal surgery, with approval from the donors and as per detailed in ethical permit 2005/1080-31/4 from Karolinska Institutet. Subjects were 61±5 years and had a BMI of 26 kg/ m^2 and no known metabolic disorders.

3.7.1 Cell culture

From the muscle biopsies, the satellite cells were isolated with trypsin and collagenase digestion. Released satellite cells were cultured to myoblasts and differentiated into myotubes with Dulbecco's modified Eagle's serum (DMEM) as described (Al-Khalili et al., 2003; Al-Khalili et al., 2004). Ham's F-10 medium, foetal bovine serum, penicillin, fungizone and streptomycin purchased from Gibco BRL (Invitrogen, Stockholm, Sweden), radioactive reagents were purchased from Amersham, all other reagents were purchased from Sigma.

3.7.2 siRNA transfection

Lipofectamine 2000 (Invitrogen) was used as transfection reagent when transfecting the cultured myotubes. Myotubes were grown on a 6-well plate and differentiation media was changed to antibiotic free media on day two of myotubes differentiation protocol. Transfections were performed on day zero and on day two with a pool of siRNAs (Dharmacon, Chicago, IL) against the human NT5C2 or scrambled sequence as a control. After transfection myotubes were washed with PBS, after which DMEM with 2% foetal bovine serum was added to each well. On day six, since the start of the differentiation, the myotubes were serum starved overnight and incubated without (basal) or with 1 mM 5-aminoimidazole-4-carboxamide-1-b-4-ribofuranoside (AICAR, from Toronto Research Chemicals Inc, Ontario Canada) before each assay.

3.7.3 mRNA expression analysis

Before RNA extraction, the myotubes were washed three times with RNase free PBS. RNeasy minikit (Qiagen). Reverse transcription was performed with the super script First Strand Synthesis System from Invitrogen. Assays were performed in duplicates in the Prism 7000 Sequence Detector using TaqMan probes from Applied Biosystems. The relative quantities of the target transcripts were calculated after data normalisation with the standard curve method. RNA from skeletal muscle biopsies were isolated using TRIZOL reagent (Invitrogen).

3.7.4 5'-nucleotide activity

Nucleotidase activity was measured as release of [^{3}H]-adenosine from 2-[^{3}H]-AMP or [^{3}H]-inosine from 8-[^{3}H]-IMP. Homogenate (20 µl) was incubated at 30°C for 15 min in 50 µl buffer containing 100 mM-Tris-HCl, 2 mM Mg-Cl_2 and 10 mM β-glycero P-Na, with either 2-[^{3}H]-AMP (200 mM, 5µCi) or 8-[^{3}H]-IMP (200 mM, 1 µCi). The addition of 10 µl 150 mM ZnSO4 and 10 µl of saturated $Ba(OH)_2$, to precipitate un-hydrolyzed AMP, terminated the incubation. Samples were placed on ice for 10 min and subjected to centrifugation at 13000 rpm at 4°C for 15 min. The radioactivity from the supernatant was determined by β- scintillation counting (Belsham *et al.*, 1980).

3.7.5 Palmitate oxidation

Lipid oxidation in myotubes was determined using [^{3}H]-palmitic acid and tritiated water was measured (Rune *et al.*, 2009). Myotubes were washed once with PBS and then incubated for 4 hours without (basal) or with 1 mM AICAR in DMEM (1 g glucose/L) media supplemented with 0.2% fatty acid free BSA and 0.5 μCi palmitic acid [9-10(n)-^{3}H]. The cell supernatant (0.2 ml) was mixed with 0.8 ml charcoal slurry (0.1 g charcoal powder in 1 ml 0.02 M tris-HCl buffer, pH 7.5) and shaken for 30 min to absorb non-metabolized palmitate. Thereafter, the samples were subjected to centrifugation at 13,000 rpm for 15 min, and radioactivity was measured from the tritium bound water in 0.2 ml of the supernatant. Samples were processed by liquid β-scintillation counting.

3.7.6 Glucose uptake

Glucose uptake was assessed in myotubes incubated for one hour without or with insulin (120 nM) or AICAR (1 mM). Myotubes were incubated in glucose-free and serum-free DMEM. Thereafter, [$^{1,2\text{-}3}$H]-2-deoxy-D-glucose (0.33 μCi/ml) and 10 μM unlabelled 2-deoxy-D-glucose was added and myotubes were incubated for a subsequent hour in glucose-free DMEM (Al-Khalili et al., 2003; Al-Khalili et al., 2004). Experiments were performed in triplicates and normalised against protein concentration (BCA Protein Assay Kit, Thermo Scientific, Rockford, IL).

3.7.7 Glucose incorporation into glycogen

The conversion of labelled glucose into glycogen was used as estimated of glycogen synthesis (Al-Khalili et al., 2003; Al-Khalili et al., 2004). Myotubes were incubated for 90 min without or with insulin (120 nM), in DMEM containing 5 mM glucose and D-[U-^{14}C] glucose (1 μCi/ml; specific activity of 0.18 Ci/mol). Experiments were performed in triplicates.

3.7.8 Glucose oxidation

Glucose oxidation was measured in myotubes incubated for four hours without or with insulin (120 nM) or AICAR (1 mM). Myotubes were incubated in DMEM containing 0.1 % fatty acid free BSA, D-[U-^{14}C] glucose (1 μCi/ml; specific activity of 0.18 Ci/mol (Amersham). 1 mM AICAR and 120 nM insulin in respective wells. Thereafter, protozol (150 μl, aqueous based tissue solubilizer, Perkin Elmer Life Science) was added to a centre-well hanging in the middle of each dish, and perchloric acid (150 μl, 35%) was added to the medium. After one hour of incubation, the centre-well was removed and subjected to scintillation counting.

3.7.9 Media lactate measurement

To measure lactate release into media from myotubes, 100 μl of media was collected in duplicates after an overnight incubation without or with AICAR (1 mM) in serum-free DMEM. The A-108 kit (Biochemical Research Service Centre, University of Buffalo, Buffalo, NY) was used to determine lactate concentrations (Bouzakri *et al.*, 2008).

3.7.10 Measurement of nucleotides

Nucleotides were measured in differentiated human myotubes and mouse *tibialis anterior* muscle. Myotubes were grown on 10 cm dishes, washed three times with ice cold PBS and scraped into 300 μl of ice cold perchloric acid (5%). The *tibialis*

anterior muscle specimens were crushed to powder in liquid nitrogen and then homogenised in 0.2 ml perchloric acid (5 %). Thereafter, the samples were subjected to centrifugation at 14,000 rpm at 4ºC for 3 min, and 0.22 ml solution of equal parts of 1 tri-n-octylamine and 1,1,2,-trichlorotrifluoroethane was added to the supernatant. The samples were vigorously mixed using a vortex. Thereafter, samples were subjected to a second round of centrifugation at the same settings as described earlier, and the upper aqueous layer was removed. To each sample, 0.22 ml of the same solution was added. Finally, 20 µl of the last aqueous phase was analysed with capillary electrophoresis and on-column isotachophoretic preconcentration, with a leading buffer (50 mM sodium phosphate, 50 mM NaCl, pH 5.2) and a tailing buffer (100 mM MES/Tris pH 5.2), hydroxyethyl-cellulose (0.2 %) added to each buffer to decrease the electro-osmotic flow. UV spectrophotometry (260 nM) was used to detect nucleotide peaks with the System Gold Software (Beckman). The peak areas were used to calculate nucleotide ratios after correction for retention time (Sakamoto *et al.*, 2005).

4 RESULTS AND DISCUSSION

To understand human diseases, and in particular T2DM, animal models are often used for studying the particular mechanism involved in the disease. Clearly animal models do not fully recapitulate the human condition and care must be taken when interpreting results from animal models (Neubauer & Kulkarni, 2006; Tkacs & Thompson, 2006). As a complementary experimental model, cell cultures may also be used. These are either commercially available cell lines or cell material from individual animals or humans. One approach is the culture of myotubes from human biopsy material, and subsequent use of these cultured myotubes for metabolic measurements. The caveat with myotubes from skeletal muscle is that they do not fully differentiate into contractile muscle when cultured and grown *in vitro*. For example, they express relatively low levels of the GLUT4 protein, and high levels of the GLUT1 protein, as compared to adult muscle. This is reflected by the different metabolic assays of cultured myotubes.

4.1 METABOLIC MEASUREMENTS ON SKELETAL MUSCLE *IN VITRO*

The experimental setup with muscles that are dissected and incubated in vials containing oxygenated solution is a common way to study metabolic pathways and drug targets (Garber *et al.*, 1976). There are, however, several important factors with this experimental setup that differ from the *in vivo* situation. Maybe the most crucial difference *in vitro* is that the muscle becomes dependent on diffusion rather than on blood flow to transfer nutrients across the cell membrane (Van Breda et al., 1990).

4.1.1 Skeletal muscle properties

In a muscle the most oxidative fibres are gathered around the largest blood vessels, which are located in the centre of the muscle. This means that the oxygen has a relatively shorter distance to cross into the oxidative fibres. This situation is reversed during *in vitro* incubation, since oxygen now has to diffuse from the outside of the muscle and hence is the most oxidative fibres are furthest away from the oxygen source (Lexell et al., 1994; Wang & Kernell, 2001; Widmer et al., 2002; Holtermann et al., 2008). In paper I, the spatial insulin signalling was investigated during *in vitro* incubation of skeletal muscle. In this analysis of the muscle it was possible to determine if insulin was able to diffuse through muscle and activate the insulin signalling cascade evenly all the way through the muscle specimen.

4.2 INSULIN SIGNALLING *IN VITRO*

The aim of paper I was to investigate whether insulin diffused throughout the whole muscle specimen during *in vitro* incubation in sufficient amounts to activate the insulin signalling cascade. The rationale behind this is a former study performed using the same *in vitro* experimental methodology (Sogaard *et al.*, 2009). The main result in the previous study was that the incubated muscles had increased protein abundance of markers for hypoxia and apoptosis (Sogaard *et al.*, 2009), together with an area of glycogen depletion in the core of the muscle (Maltin & Harris, 1985; Sogaard et al., 2009). However it could not be ruled out that the lack of glycogen in the core of the incubated muscle specimens was not due to insufficient activation of the insulin signalling cascade. As increased glucose uptake is dependent on insulin stimulation

(James *et al.*, 1988), a reduced activation of the insulin signalling pathway due to limitation in insulin diffusion could also result in a depleted area of glycogen.

As outlined in section 1.6.2, the first phosphorylated protein due to insulin stimulation is the receptor for insulin which is located in the cell membrane and is the molecule through which insulin mediates it action (De Meyts et al., 1973). The binding of insulin results in a conformational change of the IR which lowers the distance between the tyrosine kinase domains which in turn gets activated (Lee *et al.*, 1997). Each of the activated tyrosine kinase domains catalyses the phosphorylation of the other kinase domain, a process named auto-phosphorylation (Van Obberghen *et al.*, 1983). In T2DM patients, binding of insulin to IR is normal (Ciaraldi *et al.*, 2002) or impaired (Caro *et al.*, 1987). Furthermore, phosphorylation of IR have been showed to be normal (Caro et al., 1987; Krook et al., 2000) or impaired (Arner et al., 1987; Maegawa et al., 1991). The insulin signalling cascade is then perpetuated from the activated IR through PI3-K and the generation of phosphatidylinositol (3,4,5)-triphosphate to activate Akt, which is a central node in the insulin signalling cascade. Akt is also known as Protein Kinase B which is required for induction of glucose transport. Impairments in insulin signalling at the level of Akt in insulin-resistant T2DM patients have been demonstrated (Krook *et al.*, 1998). Akt works as an inhibitor of GSK3 which it phosphorylates to its inactive form, GSK3 can in its active form phosphorylate GS thereby make GS less effective. Elevated levels of GSK3α can induce insulin resistance in human skeletal muscle cells (Cross et al., 1995; Ciaraldi et al., 2007).

4.2.1 Homogenised muscle

The first measurements in paper I were performed on homogenised whole muscle samples with the multiplex detection technique Bio-Plex 200, which quantifies relative concentrations of the analytes (Jones *et al.*, 2009). The chosen analytes were pIR, pAkt and pGSK3α/β which are measures of the function of the canonical insulin signalling pathway. We provide evidence that insulin-stimulated muscle had a higher level of the phosphorylated proteins as compared to basal samples. Thus, we can conclude that insulin signalling works appropriately in the muscle specimen. However, it has to be pointed out, that by homogenising the muscle specimens, it is only the average value for the whole muscle that is measured and therefore spatial differences can be masked, as has been noted for spatial glycogen distribution (Sogaard *et al.*, 2009).

4.2.2 Sectioned muscle

From the results discussed in 4.2.1; the natural next step would be to go into the spatial resolution of the muscle specimen and assess different points in the insulin signalling cascade. We next determined whether there is a spatial heterogeneity in the canonical insulin signalling cascade following insulin-stimulation in *in vitro* incubated muscle. To assess this, we utilised immunofluorescence techniques to study transversal sections of the muscle, and measured pIR, pAkt and pGSK3α/β. We demonstrated an activation of the insulin signalling cascade throughout the muscle specimen in response to insulin stimulation. The results also indicated insulin signalling was enhanced in the centre of the muscle, specimens at the time point studied. We found this particularly interesting, since if insulin diffusion was limiting the signalling cascade, we would have expected decreases in signalling intensity towards the core of the muscle specimens. However, insulin signalling was enhanced in the centre of the muscle and we speculate that this may be due to the fact that the oxidative fibres are located more centrally in muscle specimens (Wang & Kernell, 2001) and that the oxidative fibres are more insulin sensitive (Song *et al.*, 1999). Taken together, we conclude that insulin diffusion is

sufficient to activate insulin signalling throughout the muscle specimen during *in vitro* incubation. However, as the concentration of insulin was not measured within the muscle specimens, it is not possible to conclude whether the insulin cascade was fully activated. Another possibility is to perform a time course and measure the activation of insulin signalling, however this was not performed.

4.3 KNOCK DOWN OF NT5C1A IN SKELETAL MUSCLE

In paper II was electroporation utilised to reduce protein expression of NT5C1A enzyme in *tibialis anterior* muscle of mice. In parallel, protein expression of NT5C2 enzyme was reduced in cultured human using siRNA. There are two major benefits with the electroporation system, compared with cultured myotubes. Firstly; both control and knock down conditions are studied within the same animal using contralateral muscles. In cultured myotubes, the controls come from the same origin but are grown on different plates. Secondly; the silencing is performed in an *in vivo* system such that the overall effect on metabolism may be more physiologically relevant i.e. the *in vivo* system acclimatises to the changes that the silenced protein confers, during the week until experiment is finalised.

4.3.1 Electroporation method development

Initially, the electroporation assay was conducted as described earlier (Mir *et al.*, 1999). Muscles were exposed through an incision in the skin and injected with a syringe containing the specific DNA to be electroporated. The skin was then sutured and the muscles were electroporated as described (Mir *et al.*, 1999). This method resulted in transfection efficiency of approximately 30-60% of muscle fibres when assessing the cross sectional area of the muscles 7 days after transfection (Figure 8).

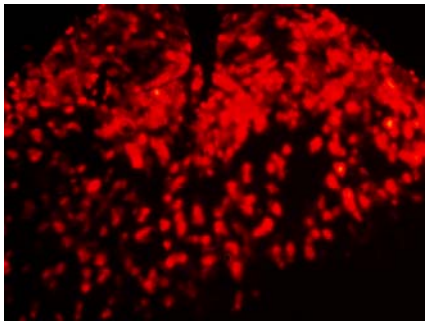

Figure 8: Transfection efficiency without the hyaluronidase pre-treatment. Electroporation performed with the pDsRed2-C1 plasmid from CLONETECH.

The second assay also followed established protocols (McMahon *et al.*, 2001). For this, the *tibialis anterior* was targeted through the skin, and because of this, an incision was unnecessary. The first step was a pre-treatment of the muscle with hyaluronidase (30 µl with 1 U/µl) for two hours before the actual injection of DNA. This step increases the transfection efficiency dramatically (McMahon *et al.*, 2001). The pre-treated animals were put back into a cage until the DNA was injected (30 µl of plasmids, 1 µg/µl), and the electrical stimulation with 220 V/cm (Figure 9). A contact gel (Ultra/Phonic Conductivity Gel by Pharmaceutical Innovations, Inc., Newark, NJ, USA), was applied to whole leg to ensure good conductivity with the calliper electrodes, square wave electrical stimulation was performed with the ECM 830 system (BTX, Harvard apparatus, Holliston, MA). There was a difference in conductivity among different brands of contact gel. The best gel for electroporation should have a conductivity of 5

mS/cm. However, since there are differences in tissue conductivity vary not only between animal strains and age, but also with the preparation of the leg before electroporation (i.e. shaving and cleaning). The gel used here (Ultra/ Phonic Conductivity Gel) had a conductivity of ~1 mS/cm as described earlier (Ivorra & Rubinsky, 2008). Thus, this gel could be regarded as in the lower range of conductivity for suitable gels.

Figure 9: Injection of *tibialis anterior* through the skin of the leg and the electrical stimulation.

Figure 10 shows the muscle pre-treated with hyaluronidase in order to get a higher transfection rate (Images are taken 7 days after electroporation). The achieved transfection rate with control plasmid (CLONTECH, pZsGreen1-C1) covered approximately 80-90% of the cross sectional area of the muscle.

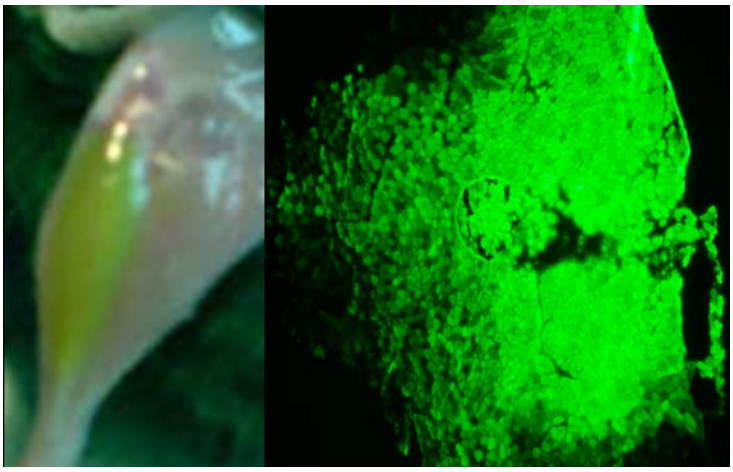

Figure 10: Transfection efficiency with hyaluronidase pre-treatment of *tibialis anterior*. Leg without skin in ordinary "room light" and cross section of the same muscle viewed in microscope. Note the fascia that divides the inner part (red/oxidative) from the other (white/glycolytic) part of *tibialis anterior*. Electroporation performed with the pZsGreen1-C1 plasmid from CLONETECH.

One caveat with this method is that the fascia in the *tibialis anterior* can work as a barrier against the injected DNA. In this case, not all of the fibres will be surrounded or bathed in DNA before the electrical stimulation. This may account for a lower expression in the inner part of the muscle (Figure 10, left part of muscle in the cross sectional picture).

4.3.2 Expression confirmation *in vivo*

The next issue was to confirm that the electroporation efficiency before sacrificing the animal, or performing an *in vivo* experiment. This expression confirmation issue was solved by using a laser pointer that concentrated all light at and into the muscle. This meant that the emission light could be observed outside the muscle (and animal) and not be disturbed by excitation light (Figure 11).

Figure 11: *In vivo* excitation of *Tibialis Anterior* transfected with the pDsRed2-C1 plasmid from CLONTECH, laser source is of 532 nm wavelength and 5 mW.

The laser source used for this purpose was of approximately the same effect as the laser in a conventional confocal microscope (5 mW and wavelength of 532 nm). The excitation light of 532 nm (green laser light) can excite a red fluorescent protein to emit red light. The pDsRed2-C1 a red fluorescent plasmid from CLONTECH was used (Figure 11). The main drawback of this expression confirmation study was that high expression of the target DNA was required to see emitted light without any extra equipment such as a whole body scan for fluorescence light. The method worked well when a transfection efficiency of approximately 50% was achieved. If the transfection efficiency was below 50%, it was challenging to see emitted light in ordinary day light.

4.3.3 Phosphorylation of AMPK and ACC

AMPK has long been regarded as a promising pharmacological target for the treatment of metabolic disease. Overexpression of an activated form of the AMPKγ3 subunit in mouse skeletal muscle has been shown to increase lipid oxidation and protect from diet-induced insulin resistance (Barnes *et al.*, 2004). AICAR is a pharmacological activator of AMPK, which has been shown to improve insulin sensitivity and glucose tolerance in diabetic animal models (Bergeron et al., 2001; Fiedler et al., 2001; Halseth et al., 2002; Song et al., 2002). AICAR is transported into the cell via the adenosine transporter. Once inside the cell, the enzyme AK transforms AICAR to 5-aminoimidazole-4-carboxamide ribonucleotide (ZMP) (Figure 2). ZMP is an analogue of AMP and the increased ratio of ZMP/ATP activates AMPK (Corton et al., 1995; Holmes et al., 1999). The disadvantage of AICAR for the treatment of metabolic disease is that it has other effects which not are linked to AMPK activation (Young *et al.*, 1996), and ZMP also activates all enzymes that are activated by AMP (Fujii *et al.*, 2006). The half-life of ZMP is also longer than the half-life of AMP since ZMP gets accumulated within the cell (Dixon *et al.*, 1991). After reducing expression of the NT5C1A enzyme by electroporation of *tibialis anterior* muscle of mice, we observed an increased phosphorylation of both AMPK and ACC by 60% and 50% respectively. Furthermore, the AMP to ATP ratio was increased 17% in NT5C1A depleted muscle (Figure 12).

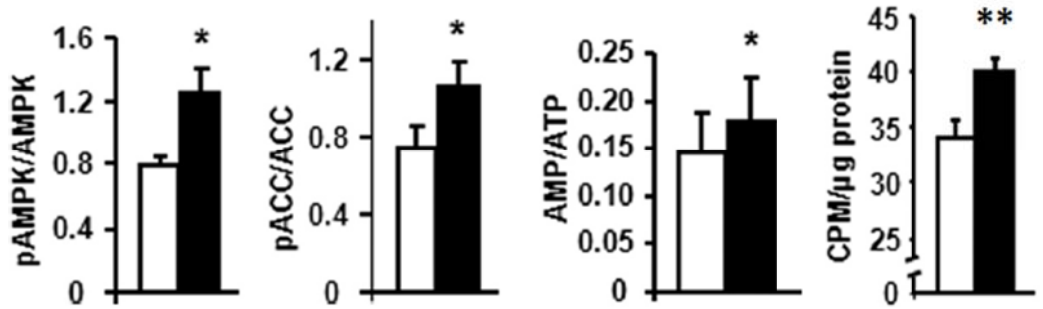

Figure 12: Silencing of NT5C1A in *tibialis anterior* increased phosphorylation of AMPK and ACC by 60% and 50% respectively. Moreover, the AMP to ATP ratio increased 17%. Collectively, these changes were associated with a 20% increase in glucose uptake. White bar refers to muscle with shRNA silencing, black bar contralateral control muscle. Results are mean±SEM. *P<0.05 versus control.

4.3.4 Glucose uptake in *tibialis anterior*

Glucose uptake was measured *in vivo*. A bolus dose of glucose (3 g/kg) was administered by gavage and thereafter radioactive labelled glucose given intraperitoneally (4.5 µl in 100 µl saline). Two hours after the glucose was administered, *tibialis anterior* muscles were dissected out and analysed. We noted a 20% increase in glucose uptake in the muscles electroporated with the shRNA NTFC1A plasmid as compared to control plasmid in contralateral muscles. This is in agreement with the increased phosphorylation of AMPK and ACC (60% and 50% respectively) measured in the same muscles (Figure 12).

4.4 NT5C2 SILENCING IN MYOTUBES

To compare the results in mouse skeletal muscle with human material, myotubes were grown from human *vastus lateralis* biopsies. In the human myotubes, the NT5C2 enzyme was silenced instead of NT5C1A. The reason for selecting a different member of the nT5C family was that NT5C1A is lowly expressed in human myotubes. The NT5C2 enzyme has a preference for GMP and IMP, but can also utilise AMP because of overlapping affinity (Banditelli *et al.*, 1996). IMP is converted by adenylosuccinate synthase into adenylosuccinate and then converted by adenylosuccinate lyase into AMP (Hatch, 1966). The NT5C2 enzyme is active over the same pathway, but with an extra intermediate step as compared to the NT5C1A enzyme. Transfection of myotubes was performed with siRNA against the NT5C2 enzyme and a scrambled sequence was used as control. The silencing resulted in a 70% reduction in protein abundance of NT5C2 (Figure 13).

4.4.1 IMP and AMP nucleotidase activity

In the NT5C2 silenced myotubes, the ratios of AMP:ATP and ADP:ATP were increased 2-fold and 3-fold, respectively. In the cytosolic fraction, the hydrolysing activity of IMP and AMP was decreased by 60% and 25%, respectively in the NT5C2 silenced myotubes. Nucleotidase activity was unaltered in the membrane fraction (paper II). These results confirm that the NT5C2 enzyme prefers IMP as substrate, but also indicate it has an overlapping affinity towards AMP (Banditelli *et al.*, 1996).

4.4.2 Phosphorylation of AMPK and ACC

NT5C2 silenced myotubes were incubated with either insulin or AICAR. In the basal state, a 2-fold increase in AMPK phosphorylation was noted. In response to AICAR, an

approximately 30% increase in AMPK phosphorylation was seen above the AICAR-stimulation in control (scrambled) cells. Similarly, ACC phosphorylation was increased 3.6-fold in the basal state, and a further increase of approximately 40% was noted after AICAR stimulation (Figure 13). Our results are in agreement with previous workers who studied AICAR stimulation (Merrill *et al.*, 1997). When comparing the results from myotubes to the results obtained from mouse *tibialis anterior* muscle, AMPK and ACC phosphorylation was greater in myotubes. Moreover, there was silencing of the target protein was increased 10% in the myotubes. The two very different experimental systems are difficult to compare, but the product of enzymatic activity is usually very responsive to number of units of the actual enzyme. According to Michaelis-Menten kinetics a difference of 10% may be of functional relevance, (Johnson & Goody, 2011).

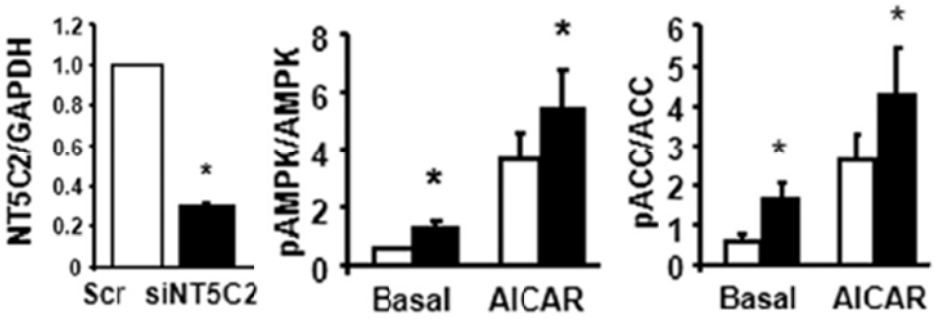

Figure 13: Silencing of NT5C2 in myotubes reduced protein abundance 70%, and increased AMPK phosphorylation 2-fold under basal conditions and 1.3-fold under AICAR-stimulated conditions. Silencing of NT5C2 also increased phosphorylation of ACC 3.6 fold under basal conditions and 1.4-fold under AICAR-stimulated conditions. White bars are scrambled and black bars are siRNA silenced myotubes. Results are mean±SEM. *P<0.05 versus control.

4.4.3 Lipid oxidation

In NT5C2 silenced myotubes, lipid oxidation was determined following insulin or AICAR stimulation. Under basal conditions, a 1.8-fold increase of lipid oxidation was noted in NT5C2 silenced myotubes. Stimulation of myotubes with insulin blunted this increase profoundly. AICAR stimulation enhanced palmitate oxidation 1.5-fold in the NT5C2 silenced myotubes as compared to the scrambled controls (Figure 14). These results are also consistent with the previously seen increased activity in the AMPK pathway in paper II.

4.4.4 Glucose uptake

The glucose uptake in the NT5C2 silenced myotubes was increased with approximately 20% under basal conditions. Insulin stimulation increased the overall uptake of glucose in both the silenced and the control state, but diminished the difference between them to an approximate 15% increase in glucose uptake in the silenced state. AICAR stimulation further increased glucose uptake compared to the basal or insulin-stimulated state, but gene silencing of NT5C2 did not altered this effect (Figure 14). Glucose incorporation to glycogen was similar between the silenced and control state, but a trend for a reduction in glucose incorporation to glycogen was noted under insulin- and AICAR-stimulated conditions for the silenced compared to control state. Glucose oxidation was unaltered between the basal, insulin and AICAR stimulated states, but a trend could be seen towards a decrease in glucose oxidation under all conditions in knock down compared to control. We noted a 22% decrease in the release of lactate from myotubes during basal state and 40% decrease under AICAR-stimulation comparing silenced to control myotubes (Figure 14).

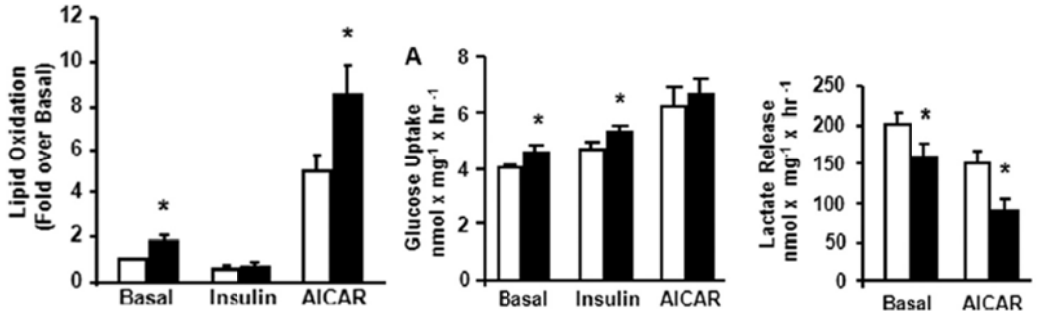

Figure 14: Silencing of NT5C2 in myotubes increased lipid oxidation under basal and AICAR-stimulated conditions by 1.8-fold and 1.5-fold, respectively. Glucose uptake was increased under basal and insulin-stimulated conditions by 20% and 15%, respectively. Lactate release decreased in both the basal and AICAR-stimulated state by 22% and 40%, respectively. Results are mean±SEM. *P<0.05 versus control.

4.5 ROLE OF THE NT5C-ENZYME IN SKELETAL MUSCLE METABOLISM

Our hypothesis that silencing the NT5C-enzyme would lead to increased phosphorylation of AMPK and ACC and also increase palmitate oxidation and glucose uptake was supported by our experimental evidence. In cultured myotubes NT5C2 silencing results in a robust increase in lipid oxidation. In contrast only a modest increase in glucose uptake was noted in myotubes following NT5C2 silencing. This is likely due to the low amount of GLUT4 expressed in the cultured myotubes as compared to skeletal muscle. Cultured muscle cells are known to only express low amounts of GLUT4 and higher amounts of GLUT1 (Al-Khalili *et al.*, 2003). Another discrepancy is that it is not possible to follow the fate of the increased glucose uptake in the other assays like glucose incorporation into glycogen, glucose oxidation or lactate release. One limitation is that the glucose uptake may only be marginally increased, and that this increase is too small to be reflected in the other assays. A second and maybe more relevant limitation is that glucose is used as tracer and the amount of glucose differs between the assays. For example, when measuring the rate of glucose uptake, [1,2-^{3}H]-2-deoxy-D-glucose was used. This was because glucose should be transported into the cell and then trapped/stopped from further metabolism. Conversely, when measuring glucose incorporation into glycogen, U-^{14}C glucose was used to allow further metabolism of glucose. The concentration of radioactively labelled glucose was 10 μM for the glucose uptake assay and 5.5 mM for the glucose oxidation assay, which is a rather big difference. Another caveat with the glucose oxidation assay was the possibility that not all of CO_2 was captured, rather only a fraction may have been trapped and this could be a reason for the discrepancy. There was also an additive effect of silencing NT5C2, which could be noted as an unexpected finding if the pathway already was maximally phosphorylated by AICAR stimulation. One reason for unexpected finding could be that NT5C2 may work as repressors of the metabolic effects of AMPK.

4.6 TBC1D1 IN SKELETAL MUSCLE METABOLISM

When TBC1D1 first was discovered, it was proposed to be involved in differentiation and cell cycle in a number of different tissues (Richardson & Zon, 1995; White et al., 2000). There are 52 proteins containing a TBC-domain in the human genome (Bernards, 2003). The TBC1D1-deficient mouse strain studied here has been shown to have increased *in vivo* fatty acid oxidation, reduced body weight, but also a reduced *in vitro* glucose uptake in the EDL muscle (Chadt *et al.*, 2008).

4.6.1 TBC1D1 in humans

A R125W mutation in TBC1D1 has been linked to a predisposition for severe obesity in humans (Stone *et al.*, 2006). Increased risk of T2DM has also been linked to TBC1D1 via single-nucleotide polymorphism (SNP) hits in the TBC1D1 domain (Zeggini *et al.*, 2007). The R125W mutation is located in the phosphotyrosine-binding site, which is involved in protein-protein interaction (Stone *et al.*, 2006). Overexpression of the R125W mutant by electroporation in mice decreased insulin-stimulated glucose uptake (An *et al.*, 2010). Since TBC1D1 is an Akt substrate, and is inactivated in its phosphorylated state, the R125W mutation might prevent Akt from phosphorylating TBC1D1, and prevent inactivation. This would result in a constitutively active GAP domain, which in turn would act as a brake on GLUT4 translocation via the inactivation of Rab-GTP to Rab-GDP.

4.6.2 TBC1D1 insulin-stimulated glucose uptake

The TBC1D1-deficient mouse strain studied here would hypothetically not have a brake on GLUT4 translocation because the TBC1D1 protein with the GAP-domain which makes the inactive form of Rab (Rab-GDP) is not produced. The expected phenotype of the TBC1D1-deficient mouse would be an increased rate of glucose uptake and fatty acid oxidation in the muscles in which TBC1D1 is endogenously expressed.

4.6.3 Clamp method development

In the original clamp surgery, the visible end of the catheter was placed through a plastic stopper that was in turn placed in an incision made on the neck of the mouse. The extra length of the catheter was placed under the skin towards the tail, and on the day of experiment the catheter was pulled out through the plastic stopper (approximately 10 cm) and connected to the infusion pump. This sometimes resulted in attachment of the catheter as the incision healed and inflammation at the protruding end of the catheter. In some cases when inflammation was noted, the animal failed to gain weight during the recovery week. To avoid this, the surgery was modified as follows: the skin itself was used as a stopper, instead of the plastic stopper. This was possible because the catheter already had a small stopper attached. Hence the incision for handling the catheter was made on the side of the neck, and on top of the neck (where the previous incision would have been) a small skin puncture was made so that the catheter could fit through (Figure 15).

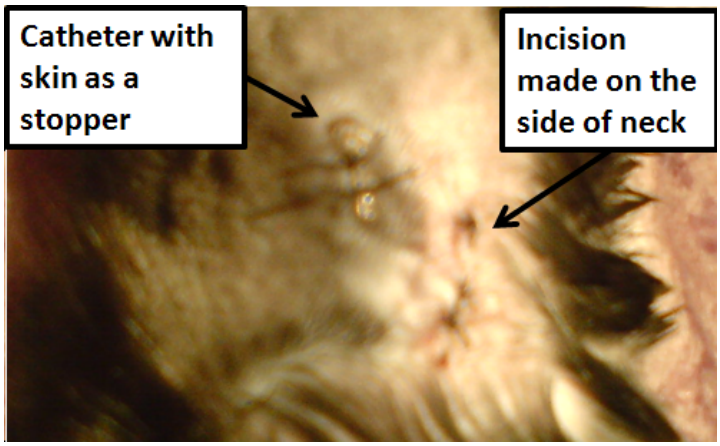

Figure 15: Clamp surgery with incision on the side of the neck, and the skin used as stopper for catheter.

With this modification, the incision healed nicely and the mice were not irritated by the catheter. This resulted in a post-surgery weight gain 0.5-1.5 grams between the surgery and the actual day of the experiment (1 week). With the old protocol, the mice remained at the same weight or actually lost weight during the post-surgery phase. The modified surgery was associated with increase in glucose uptake in skeletal muscle during 2-DOG clamp (Figure 16).

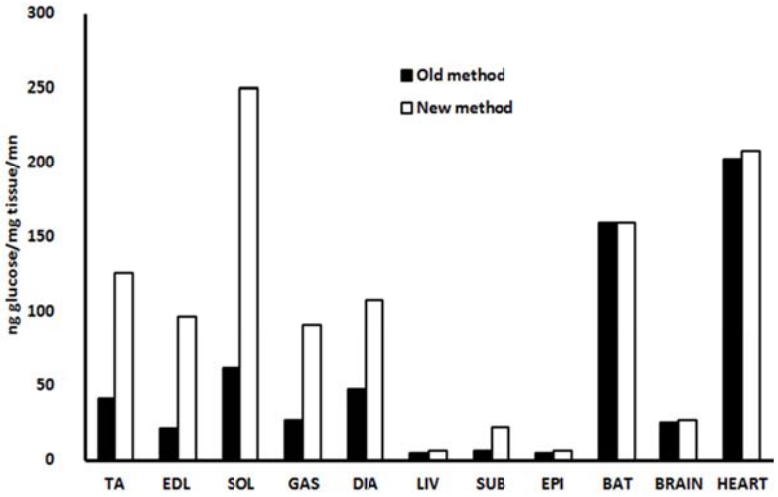

Figure 16: Difference in glucose uptake during 2-DOG clamp using the old method (black bars) versus new method (white bars) for surgery. Results are reported as mean values for n=3 (old method) and n=7 (new method) mice.

4.6.4 Clamp metabolic measurements

The improved clamp technique was used to assess tissue specific glucose uptake using the 2-DOG. GTR was assessed by the euglycemic hyperinsulinemic clamp, where it is possible to assess the insulin sensitivity of the liver as well as the peripheral tissues. The GTR clamp shows that TBC1D1 knock out animals have higher liver sensitivity to insulin compared to wild type, but peripheral sensitivity is unaltered. The 2DOG clamp shows that insulin-stimulated glucose uptake is higher in the *tibialis anterior* and EDL muscle. These muscles have a higher endogenous expression of the TBC1D1 protein compared to the *soleus* and gastrocnemius which did not show any significant difference in insulin-stimulated glucose uptake. The results indicate that TBC1D1 has an important role in the insulin-stimulated glucose uptake in skeletal muscle.

4.6.5 Capillary staining

In order to assess the number of capillaries per muscle fibre and number of fibres per square millimetre of whole muscle specimen, a indoxyl-tetrazolium method for alkaline phosphatase was used to permanently stain the enzyme in the capillary endothelium **(Ziada et al., 1984).** An example of the capillary staining of *tibialis anterior*, EDL and *soleus* can be viewed in Figure 17.

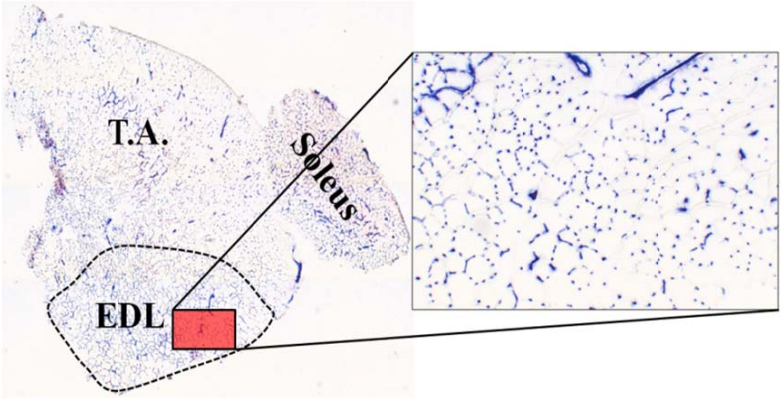

Figure 17: Example of alkaline phosphatase staining of capillaries in *tibialis anterior*, *soleus* and EDL.

The number of capillaries per fibre was counted manually from the picture seen in figure 17. The total number of capillaries per square millimetre of muscle was analysed using the Image-J (http://rsbweb.nih.gov/ij/) program. Pictures were processed as mentioned in methods and the binary picture was used for measuring capillaries per square millimetre (figure 18).

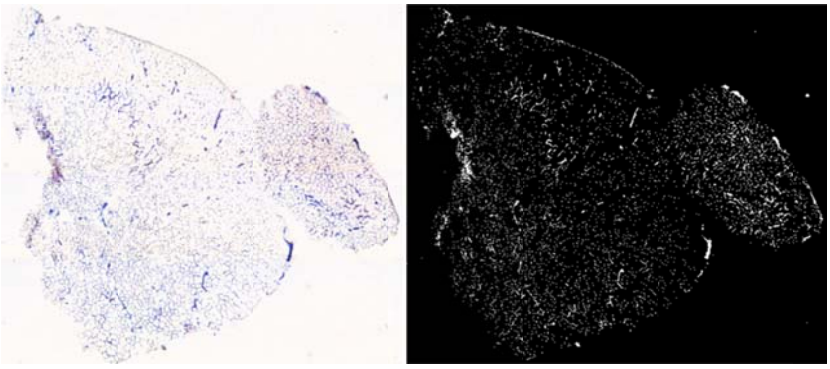

Figure 18: Example of image before and after processing. To visualise and count the number of capillaries, the Image-j freeware program was used to process image.

Capillary assessment reveals similar number of capillaries per muscle fibre and number of fibres per square millimetre between the TBC1D1 knock-out and the wild-type mice.

4.7 SUMMARY OF FINDINGS

The main focus of this thesis is the regulation of glucose uptake in skeletal muscle (Figure 19). The main findings of the different papers are summarised below:

- In paper I, we characterised the insulin signalling cascade in *in vitro* incubated skeletal muscle. Specifically, we noted that insulin sufficiently diffuses into the centre of tubular mouse muscles to promote phosphorylation of these signalling events. Moreover, insulin signalling is increased in the core of the incubated muscle specimens, correlating with the location of oxidative fibres.

- In paper II we validated the role of NT5C enzymes in the regulation of glucose and lipid metabolism. We provide evidence that gene silencing of NT5C enzymes increases the AMP/ATP ratio and this is associated with increased phosphorylation of AMPK and ACC. These changes in signal transduction are associated with increased glucose uptake and fatty acid oxidation.

- In paper III, we investigated the metabolic role of TBC1D1 in skeletal muscle metabolism. We provide evidence that the Rab-GTPase activating protein TBC1D1 is involved in metabolic regulation and that functional TBC1D1 is required for AICAR- and contraction-induced *in vitro* metabolic responses, implicating a role in energy-sensing signals. We show that TBC1D1-deficiency increases insulin-stimulated glucose uptake in *tibialis anterior* and EDL muscle during 2-DOG clamp. TBC1D1-deficiency also gives increased hepatic insulin sensitivity during the GTR clamp.

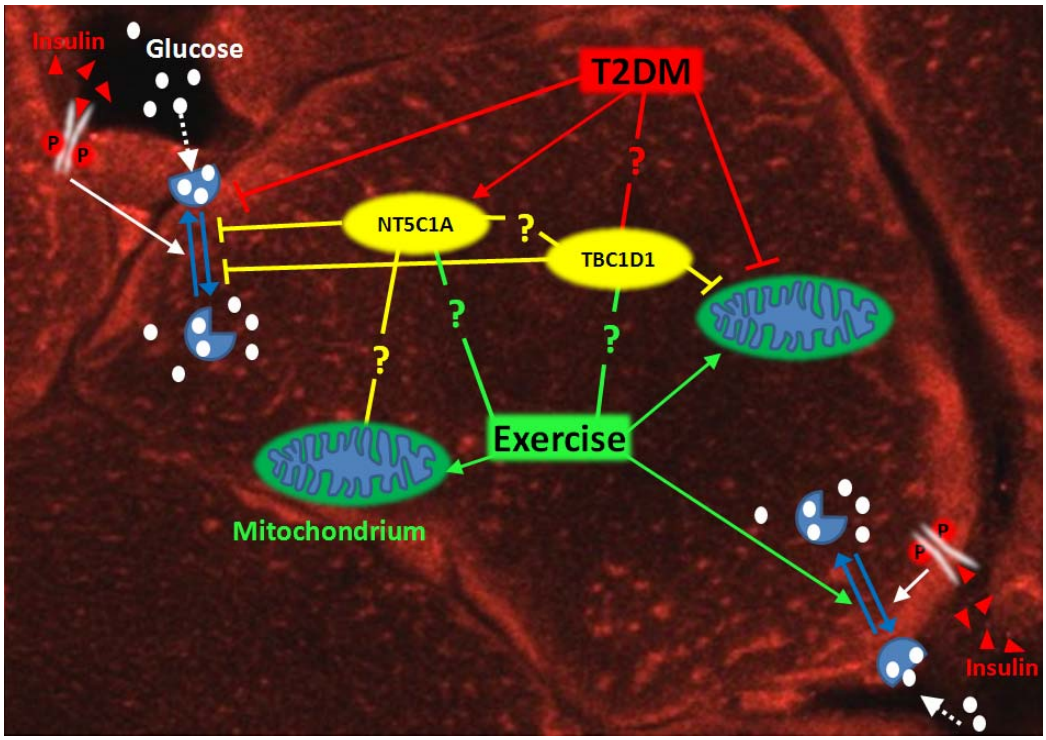

Figure 19: The main pathways studied in this thesis. The NT5C1A protein was found to be a negative regulator of insulin-stimulated glucose uptake and fatty acid oxidation. TBC1D1 has a negative effect on glucose uptake and on fatty acid oxidation.

5 CONCLUSIONS AND FURTHER PERSPECTIVES

In this thesis work, new data regarding insulin signalling and molecular targets controlling metabolism have been revealed. Specific conclusions of each study include the following:

Paper I: Insulin action is not restricted in isolated skeletal muscle preparations due to insufficient diffusion of the hormone during *in vitro* incubation. Thus, isolated skeletal muscle preparations are a viable technique to study the acute effects of insulin on signal transduction.

Paper II: Endogenous expression of NT5C enzymes is likely to inhibit basal lipid oxidation and glucose transport in skeletal muscle. Thus, pharmacological approaches to reduce 5'-nucleotidase expression or activity may promote metabolic flexibility in type 2 diabetes mellitus.

Paper III: TBC1D1 protein is linked to the regulation of GLUT4 protein and glucose uptake in skeletal muscle. Enhanced hepatic insulin sensitivity and enhanced glucose homeostasis in glycolytic muscle from TBC1D1-deficient mice supports the role of TBC1D1 as a Rab-GTPase activating protein. Thus, functional TBC1D1 is required for contraction and AICAR responses *in vitro*, which suggests that TBC1D1 is involved in sensing or regulation of oxidative pathways.

The overarching conclusion of this thesis is that molecular pathways controlling glucose uptake in skeletal muscle are important to understand to eventually prevent and treat T2DM. We conclude that insulin signalling is functional in the *in vitro* incubated skeletal muscle specimens. Moreover, the molecular switches TBC1D1 and NT5C1A have high impact on glucose uptake in skeletal muscle. The results presented in this thesis may impact the understanding of metabolic pathways contributing to the development of insulin resistance in T2DM

Future studies to investigate whether there is a connection between NT5C1A and exercise training and whether NT5C1A enzymes impact mitochondria function may be warranted. In addition, future studies to determine the whether TBC1D1 is altered in skeletal muscle from people with T2DM or after exercise training are of interest. Other work may be directed towards understanding whether there is an internal relationship between NT5C1A and TBC1D1. Another perspective is pursuing the possibility to use the NT5C1A enzyme and the nucleosides as molecular marker for metabolic status in T2DM patients. The concept of using nucleosides as molecular marker is already being used in case of cancer and liver diseases.

6 ACKNOWLEDGEMENTS

I would like to express my gratitude to all the people that I have encountered during this work, and especially to:

My main supervisor Professor **Juleen R. Zierath**, for the opportunity to work in this group and for making this work possible. For invaluable guidance and for teaching me the many aspects of science.

My co-supervisor Professor **Anna Krook,** for great knowledge and always being positive and easy to talk to.

To my mentor Dr. **Erik Walum** for invaluable discussions and guidance, time goes to fast.

Dr. **Peter Sögård** for team work, friendship and great discussions, but especially for introducing me to Karolinska Institutet.

All present and former colleagues and friends at the Integrative Physiology group, which made these years of work interesting and motivating. ***Thank you!***

I would like to especially acknowledge: Docent **Pablo Garcia-Roves** for great scientific expertise and for always being helpful and for friendship. Professor **Marc Gilbert** for guidance and help with surgery and clamp experiments. Docent **Alexander V. Chibalin** for expertise, patience and good advice. Dr. **Håkan Karlsson** for help and great discussions, both in science and other areas. Dr. **Dana Galuska** for always helping out with long forgotten assays. **Robby Zachariah Tom** for invaluable help in the laboratory and friendship. Dr. **Boubacar Benziane** for friendship and guidance in cell work. Dr. **Reginald L. Austin** for great friendship and words of wisdom. Dr. **Firoozeh Salehzadeh** for friendship great discussion and advice. Dr. **Brendan Egan** for interesting discussions and friendship. Dr. **Julie Massart** for friendship and help with bench work. Dr. **Dorit Schleinitz** for friendship and interesting discussions. Dr. **Eduardo Iglesias** for friendship and scientific discussions. MD. **Fredirick Mashili** for interesting experiments and friendship. Dr. **Atul S. Deshmukh** and **Sameer Kulkarni** for collaboration and interesting experiments. Dr. **Megan Osler** for introducing me into field of immunofluorescence. Dr. **Lake Qunfeng Jiang** for the introduction to plasmid cloning and answering my many questions. Dr. **Marie Björnholm** for assistance, support and for guidance with animal experiments. Dr. **Stephan Glund** for great scientific discussions. Dr. **Asuka Naito** and Dr. **Naoki Miyoshi** for great knowledge and interesting scientific discussions. **Margareta Svedlund** for always being supportive and for great administrative assistance.

Special thanks to the animal department staff for always being helpful and for professional animal care.

I would also like to thank collaborators and friends outside the Integrative Physiology group: Professor **Anders Arner** for invaluable help with contraction, confocal imaging and great scientific knowledge. **Mirjana Poljakovic** for help with confocal experiments. Professor **Barbara Canlon** and **Agneta Viberg** for invaluable help, guidance and microscopical assistance. **Frida Eiengård** for friendship and great times. **Raquel Domingo Fernández** for friendship and for believing in me. **Niclas Janson** and **Jonathan Holmén** for friendship and great times. **Louise Bovin** for friendship and guidance in Stockholm. Dr. **Takashi Yamada** for interesting discussions and friendship. Dr. **Alexandra Chadt** for great discussions, interesting experiments and words of wisdom. **Eva-Karin Sällstedt** for help with protocol and good advice.

Professor **Stefano Schiaffino** Dr. **Marta Murgia** and co-workers at the University of Padova, for professional guidance in the field of electroporation and interesting scientific discussions.

Speciellt skulle jag vilja tacka min familj:
Mina föräldar **Ferenc** och **Märta Szekeres** för eran kärlek, ert stöd och förtroende som jag alltid kan lita på.
Min bror **Per-Åke Szekeres**, **Jenny Arenblad**, **Oliva** och **Zelma Szekeres** för allt roligt vi haft och allt roligt som komma skall.

私は思い出にはならないさ

7 REFERENCES

Al-Khalili, L., Chibalin, A. V., Kannisto, K., Zhang, B. B., Permert, J., Holman, G. D., Ehrenborg, E., Ding, V. D., Zierath, J. R., Krook, A. 2003. Insulin action in cultured human skeletal muscle cells during differentiation: assessment of cell surface GLUT4 and GLUT1 content. *Cell Mol Life Sci*, 60(5): 991-998.

Al-Khalili, L., Kramer, D., Wretenberg, P., Krook, A. 2004. Human skeletal muscle cell differentiation is associated with changes in myogenic markers and enhanced insulin-mediated MAPK and PKB phosphorylation. *Acta Physiol Scand*, 180(4): 395-403.

Alberti, K. G., Zimmet, P. Z. 1998. Definition, diagnosis and classification of diabetes mellitus and its complications. Part 1: diagnosis and classification of diabetes mellitus provisional report of a WHO consultation. *Diabet Med*, 15(7): 539-553.

An, D., Toyoda, T., Taylor, E. B., Yu, H., Fujii, N., Hirshman, M. F., Goodyear, L. J. 2010. TBC1D1 regulates insulin- and contraction-induced glucose transport in mouse skeletal muscle. *Diabetes*, 59(6): 1358-1365.

Arner, P., Pollare, T., Lithell, H., Livingston, J. N. 1987. Defective insulin receptor tyrosine kinase in human skeletal muscle in obesity and type 2 (non-insulin-dependent) diabetes mellitus. *Diabetologia*, 30(6): 437-440.

Banditelli, S., Baiocchi, C., Pesi, R., Allegrini, S., Turriani, M., Ipata, P. L., Camici, M., Tozzi, M. G. 1996. The phosphotransferase activity of cytosolic 5'-nucleotidase; a purine analog phosphorylating enzyme. *Int J Biochem Cell Biol*, 28(6): 711-720.

Banting, F. G., Best, C. H., Collip, J. B., Campbell, W. R., Fletcher, A. A. 1922. Pancreatic Extracts in the Treatment of Diabetes Mellitus. *Can Med Assoc J*, 12(3): 141-146.

Barnes, B. R., Marklund, S., Steiler, T. L., Walter, M., Hjalm, G., Amarger, V., Mahlapuu, M., Leng, Y., Johansson, C., Galuska, D., Lindgren, K., Abrink, M., Stapleton, D., Zierath, J. R., Andersson, L. 2004. The 5'-AMP-activated protein kinase gamma3 isoform has a key role in carbohydrate and lipid metabolism in glycolytic skeletal muscle. *J Biol Chem*, 279(37): 38441-38447.

Baron, A. D., Brechtel, G., Wallace, P., Edelman, S. V. 1988. Rates and tissue sites of non-insulin- and insulin-mediated glucose uptake in humans. *Am J Physiol*, 255(6 Pt 1): E769-774.

Belsham, G. J., Denton, R. M., Tanner, M. J. 1980. Use of a novel rapid preparation of fat-cell plasma membranes employing Percoll to investigate the effects of insulin and adrenaline on membrane protein phosphorylation within intact fat-cells. *Biochem J*, 192(2): 457-467.

Bergeron, R., Previs, S. F., Cline, G. W., Perret, P., Russell, R. R., 3rd, Young, L. H., Shulman, G. I. 2001. Effect of 5-aminoimidazole-4-carboxamide-1-beta-D-ribofuranoside infusion on in vivo glucose and lipid metabolism in lean and obese Zucker rats. *Diabetes*, 50(5): 1076-1082.

Bernards, A. 2003. GAPs galore! A survey of putative Ras superfamily GTPase activating proteins in man and Drosophila. *Biochim Biophys Acta*, 1603(2): 47-82.

Birnbaum, M. J. 1989. Identification of a novel gene encoding an insulin-responsive glucose transporter protein. *Cell*, 57(2): 305-315.

Bjorntorp, P., Sjostrom, L. 1978. Carbohydrate storage in man: speculations and some quantitative considerations. *Metabolism*, 27(12 Suppl 2): 1853-1865.

Boden, G., Chen, X. 1995. Effects of fat on glucose uptake and utilization in patients with non-insulin-dependent diabetes. *J Clin Invest*, 96(3): 1261-1268.

Bouzakri, K., Austin, R., Rune, A., Lassman, M. E., Garcia-Roves, P. M., Berger, J. P., Krook, A., Chibalin, A. V., Zhang, B. B., Zierath, J. R. 2008. Malonyl CoenzymeA decarboxylase regulates lipid and glucose metabolism in human skeletal muscle. *Diabetes*, 57(6): 1508-1516.

Brechtel, K., Dahl, D. B., Machann, J., Bachmann, O. P., Wenzel, I., Maier, T., Claussen, C. D., Haring, H. U., Jacob, S., Schick, F. 2001. Fast elevation of the intramyocellular lipid content in the presence of circulating free fatty acids and hyperinsulinemia: a dynamic 1H-MRS study. *Magn Reson Med*, 45(2): 179-183.

Careddu, M. G., Allegrini, S., Pesi, R., Camici, M., Garcia-Gil, M., Tozzi, M. G. 2008. Knockdown of cytosolic 5'-nucleotidase II (cN-II) reveals that its activity is essential for survival in astrocytoma cells. *Biochim Biophys Acta*, 1783(8): 1529-1535.

Caro, J. F., Sinha, M. K., Raju, S. M., Ittoop, O., Pories, W. J., Flickinger, E. G., Meelheim, D., Dohm, G. L. 1987. Insulin receptor kinase in human skeletal muscle from obese subjects with and without noninsulin dependent diabetes. *J Clin Invest*, 79(5): 1330-1337.

Cartee, G. D., Dean, D. J. 1994. Glucose transport with brief dietary restriction: heterogenous responses in muscles. *Am J Physiol*, 266(6 Pt 1): E946-952.

Chadt, A., Leicht, K., Deshmukh, A., Jiang, L. Q., Scherneck, S., Bernhardt, U., Dreja, T., Vogel, H., Schmolz, K., Kluge, R., Zierath, J. R., Hultschig, C., Hoeben, R. C., Schurmann, A., Joost, H. G., Al-Hasani, H. 2008. Tbc1d1 mutation in lean mouse strain confers leanness and protects from diet-induced obesity. *Nat Genet*, 40(11): 1354-1359.

Ciaraldi, T. P., Carter, L., Rehman, N., Mohideen, P., Mudaliar, S., Henry, R. R. 2002. Insulin and insulin-like growth factor-1 action on human skeletal muscle: preferential effects of insulin-like growth factor-1 in type 2 diabetic subjects. *Metabolism*, 51(9): 1171-1179.

Ciaraldi, T. P., Nikoulina, S. E., Bandukwala, R. A., Carter, L., Henry, R. R. 2007. Role of glycogen synthase kinase-3 alpha in insulin action in cultured human skeletal muscle cells. *Endocrinology*, 148(9): 4393-4399.

Cline, G. W., Petersen, K. F., Krssak, M., Shen, J., Hundal, R. S., Trajanoski, Z., Inzucchi, S., Dresner, A., Rothman, D. L., Shulman, G. I. 1999. Impaired glucose transport as a cause of decreased insulin-stimulated muscle glycogen synthesis in type 2 diabetes. *N Engl J Med*, 341(4): 240-246.

Cordain, L., Miller, J. B., Eaton, S. B., Mann, N., Holt, S. H., Speth, J. D. 2000. Plant-animal subsistence ratios and macronutrient energy estimations in worldwide hunter-gatherer diets. *Am J Clin Nutr*, 71(3): 682-692.

Corton, J. M., Gillespie, J. G., Hawley, S. A., Hardie, D. G. 1995. 5-aminoimidazole-4-carboxamide ribonucleoside. A specific method for activating AMP-activated protein kinase in intact cells? *Eur J Biochem*, 229(2): 558-565.

Cross, D. A., Alessi, D. R., Cohen, P., Andjelkovich, M., Hemmings, B. A. 1995. Inhibition of glycogen synthase kinase-3 by insulin mediated by protein kinase B. *Nature*, 378(6559): 785-789.

Cushman, S. W., Wardzala, L. J. 1980. Potential mechanism of insulin action on glucose transport in the isolated rat adipose cell. Apparent translocation of intracellular transport systems to the plasma membrane. *J Biol Chem*, 255(10): 4758-4762.

De Meyts, P., Roth, J., Neville, D. M., Jr., Gavin, J. R., 3rd, Lesniak, M. A. 1973. Insulin interactions with its receptors: experimental evidence for negative cooperativity. *Biochem Biophys Res Commun*, 55(1): 154-161.

DeFronzo, R., Deibert, D., Hendler, R., Felig, P., Soman, V. 1979a. Insulin sensitivity and insulin binding to monocytes in maturity-onset diabetes. *J Clin Invest*, 63(5): 939-946.

DeFronzo, R. A. 1988. Obesity is associated with impaired insulin-mediated potassium uptake. *Metabolism*, 37(2): 105-108.

DeFronzo, R. A. 2010. Current issues in the treatment of type 2 diabetes. Overview of newer agents: where treatment is going. *Am J Med*, 123(3 Suppl): S38-48.

DeFronzo, R. A., Gunnarsson, R., Bjorkman, O., Olsson, M., Wahren, J. 1985. Effects of insulin on peripheral and splanchnic glucose metabolism in noninsulin-dependent (type II) diabetes mellitus. *J Clin Invest*, 76(1): 149-155.

DeFronzo, R. A., Tobin, J. D., Andres, R. 1979b. Glucose clamp technique: a method for quantifying insulin secretion and resistance. *Am J Physiol*, 237(3): E214-223.

Dixon, R., Gourzis, J., McDermott, D., Fujitaki, J., Dewland, P., Gruber, H. 1991. AICA-riboside: safety, tolerance, and pharmacokinetics of a novel adenosine-regulating agent. *J Clin Pharmacol*, 31(4): 342-347.

Edgerton, D. S., Johnson, K. M., Cherrington, A. D. 2009. Current strategies for the inhibition of hepatic glucose production in type 2 diabetes. *Front Biosci*, 14: 1169-1181.

Fiedler, M., Zierath, J. R., Selen, G., Wallberg-Henriksson, H., Liang, Y., Sakariassen, K. S. 2001. 5-aminoimidazole-4-carboxy-amide-1-beta-D-ribofuranoside treatment ameliorates hyperglycaemia and hyperinsulinaemia but not dyslipidaemia in KKAy-CETP mice. *Diabetologia*, 44(12): 2180-2186.

Fujii, N., Jessen, N., Goodyear, L. J. 2006. AMP-activated protein kinase and the regulation of glucose transport. *Am J Physiol Endocrinol Metab*, 291(5): E867-877.

Fukumoto, H., Kayano, T., Buse, J. B., Edwards, Y., Pilch, P. F., Bell, G. I., Seino, S. 1989. Cloning and characterization of the major insulin-responsive glucose transporter expressed in human skeletal muscle and other insulin-responsive tissues. *J Biol Chem*, 264(14): 7776-7779.

Garber, A. J., Karl, I. E., Kipnis, D. M. 1976. Alanine and glutamine synthesis and release from skeletal muscle. I. Glycolysis and amino acid release. *J Biol Chem*, 251(3): 826-835.

Gazziola, C., Ferraro, P., Moras, M., Reichard, P., Bianchi, V. 2001. Cytosolic high K(m) 5'-nucleotidase and 5'(3')-deoxyribonucleotidase in substrate cycles involved in nucleotide metabolism. *J Biol Chem*, 276(9): 6185-6190.

Gibson, W. B., Drummond, G. I. 1972. Properties of 5'-nucleotidase from avian heart. *Biochemistry*, 11(2): 223-229.

Habinowski, S. A., Hirshman, M., Sakamoto, K., Kemp, B. E., Gould, S. J., Goodyear, L. J., Witters, L. A. 2001. Malonyl-CoA decarboxylase is not a substrate of AMP-activated protein kinase in rat fast-twitch skeletal muscle or an islet cell line. *Arch Biochem Biophys*, 396(1): 71-79.

Halseth, A. E., Ensor, N. J., White, T. A., Ross, S. A., Gulve, E. A. 2002. Acute and chronic treatment of ob/ob and db/db mice with AICAR decreases blood glucose concentrations. *Biochem Biophys Res Commun*, 294(4): 798-805.

Hanisch, F., Hellsten, Y., Zierz, S. 2006. Ecto- and cytosolic 5'-nucleotidases in normal and AMP deaminase-deficient human skeletal muscle. *Biol Chem*, 387(1): 53-58.

Hardie, D. G., Salt, I. P., Hawley, S. A., Davies, S. P. 1999. AMP-activated protein kinase: an ultrasensitive system for monitoring cellular energy charge. *Biochem J*, 338 (Pt 3): 717-722.

Hatch, M. D. 1966. Adenylosuccinate synthetase and adenylosuccinate lyase from plant tissues. *Biochem J*, 98(1): 198-203.

Holloszy, J. O., Hansen, P. A. 1996. Regulation of glucose transport into skeletal muscle. *Rev Physiol Biochem Pharmacol*, 128: 99-193.

Holmes, B. F., Kurth-Kraczek, E. J., Winder, W. W. 1999. Chronic activation of 5'-AMP-activated protein kinase increases GLUT-4, hexokinase, and glycogen in muscle. *J Appl Physiol*, 87(5): 1990-1995.

Holtermann, A., Gronlund, C., Stefan Karlsson, J., Roeleveld, K. 2008. Spatial distribution of active muscle fibre characteristics in the upper trapezius muscle and its dependency on contraction level and duration. *J Electromyogr Kinesiol*, 18(3): 372-381.

Hunsucker, S. A., Mitchell, B. S., Spychala, J. 2005. The 5'-nucleotidases as regulators of nucleotide and drug metabolism. *Pharmacol Ther*, 107(1): 1-30.

Ilanne-Parikka, P., Eriksson, J. G., Lindstrom, J., Peltonen, M., Aunola, S., Hamalainen, H., Keinanen-Kiukaanniemi, S., Laakso, M., Valle, T. T., Lahtela, J., Uusitupa, M., Tuomilehto, J. 2008. Effect of lifestyle intervention on the occurrence of metabolic syndrome and its components in the Finnish Diabetes Prevention Study. *Diabetes Care*, 31(4): 805-807.

Ivorra, A., Rubinsky, B. 2008. Optimum Conductivity of Gels for Electric Field Homogenization in Tissue Electroporation Therapies. *Iv Latin American Congress on Biomedical Engineering 2007, Bioengineering Solutions for Latin America Health, Vols 1 and 2*, 18(1,2): 619-622.

James, D. E., Brown, R., Navarro, J., Pilch, P. F. 1988. Insulin-regulatable tissues express a unique insulin-sensitive glucose transport protein. *Nature*, 333(6169): 183-185.

Jensen, J., Jebens, E., Brennesvik, E. O., Ruzzin, J., Soos, M. A., Engebretsen, E. M., O'Rahilly, S., Whitehead, J. P. 2006. Muscle glycogen inharmoniously regulates glycogen synthase activity, glucose uptake, and proximal insulin signaling. *Am J Physiol Endocrinol Metab*, 290(1): E154-E162.

Jensen, J., Lai, Y. C. 2009. Regulation of muscle glycogen synthase phosphorylation and kinetic properties by insulin, exercise, adrenaline and role in insulin resistance. *Arch Physiol Biochem*, 115(1): 13-21.

Johnson, K. A., Goody, R. S. 2011. The original Michaelis constant: translation of the 1913 Michaelis-Menten paper. *Biochemistry*, 50(39): 8264-8269.

Jones, R. J., Young, O., Renshaw, L., Jacobs, V., Fennell, M., Marshall, A., Green, T. P., Elvin, P., Womack, C., Clack, G., Dixon, J. M. 2009. Src inhibitors in early breast cancer: a methodology, feasibility and variability study. *Breast Cancer Res Treat*, 114(2): 211-221.

Kahn, C. R., Neville, D. M., Jr., Gorden, P., Freychet, P., Roth, J. 1972. Insulin receptor defect in insulin resistance: studies in the obese-hyperglycimic mouse. *Biochem Biophys Res Commun*, 48(1): 135-142.

Kahn, C. R., White, M. F. 1988. The insulin receptor and the molecular mechanism of insulin action. *J Clin Invest*, 82(4): 1151-1156.

Kane, S., Sano, H., Liu, S. C., Asara, J. M., Lane, W. S., Garner, C. C., Lienhard, G. E. 2002. A method to identify serine kinase substrates. Akt phosphorylates a novel adipocyte protein with a Rab GTPase-activating protein (GAP) domain. *J Biol Chem*, 277(25): 22115-22118.

Kelley, D. E., Wing, R., Buonocore, C., Sturis, J., Polonsky, K., Fitzsimmons, M. 1993. Relative effects of calorie restriction and weight loss in noninsulin-dependent diabetes mellitus. *J Clin Endocrinol Metab*, 77(5): 1287-1293.

Kim, J. K. 2009. Hyperinsulinemic-euglycemic clamp to assess insulin sensitivity in vivo. *Methods Mol Biol*, 560: 221-238.

Kolaczynski, J. W., Caro, J. F. 1998. Insulin resistance: site of the primary defect or how the current and the emerging therapies work. *J Basic Clin Physiol Pharmacol*, 9(2-4): 281-294.

Krook, A., Bjornholm, M., Galuska, D., Jiang, X. J., Fahlman, R., Myers, M. G., Jr., Wallberg-Henriksson, H., Zierath, J. R. 2000. Characterization of signal transduction and glucose transport in skeletal muscle from type 2 diabetic patients. *Diabetes*, 49(2): 284-292.

Krook, A., Roth, R. A., Jiang, X. J., Zierath, J. R., Wallberg-Henriksson, H. 1998. Insulin-stimulated Akt kinase activity is reduced in skeletal muscle from NIDDM subjects. *Diabetes*, 47(8): 1281-1286.

Lee, A. D., Hansen, P. A., Holloszy, J. O. 1995. Wortmannin inhibits insulin-stimulated but not contraction-stimulated glucose transport activity in skeletal muscle. *FEBS Lett*, 361(1): 51-54.

Lee, J., Pilch, P. F., Shoelson, S. E., Scarlata, S. F. 1997. Conformational changes of the insulin receptor upon insulin binding and activation as monitored by fluorescence spectroscopy. *Biochemistry*, 36(9): 2701-2708.

Lexell, J., Jarvis, J. C., Currie, J., Downham, D. Y., Salmons, S. 1994. Fibre type composition of rabbit tibialis anterior and extensor digitorum longus muscles. *J Anat*, 185 (Pt 1): 95-101.

Maegawa, H., Shigeta, Y., Egawa, K., Kobayashi, M. 1991. Impaired autophosphorylation of insulin receptors from abdominal skeletal muscles in nonobese subjects with NIDDM. *Diabetes*, 40(7): 815-819.

Maltin, C. A., Harris, C. I. 1985. Morphological observations and rates of protein synthesis in rat muscles incubated in vitro. *Biochem J*, 232(3): 927-930.

McGarry, J. D. 1995. The mitochondrial carnitine palmitoyltransferase system: its broadening role in fuel homoeostasis and new insights into its molecular features. *Biochem Soc Trans*, 23(2): 321-324.

McMahon, J. M., Signori, E., Wells, K. E., Fazio, V. M., Wells, D. J. 2001. Optimisation of electrotransfer of plasmid into skeletal muscle by pretreatment with hyaluronidase -- increased expression with reduced muscle damage. *Gene Ther*, 8(16): 1264-1270.

McMahon, J. M., Wells, D. J. 2004. Electroporation for gene transfer to skeletal muscles: current status. *BioDrugs*, 18(3): 155-165.

Merrill, G. F., Kurth, E. J., Hardie, D. G., Winder, W. W. 1997. AICA riboside increases AMP-activated protein kinase, fatty acid oxidation, and glucose uptake in rat muscle. *Am J Physiol*, 273(6 Pt 1): E1107-1112.

Mikines, K. J., Sonne, B., Tronier, B., Galbo, H. 1989. Effects of acute exercise and detraining on insulin action in trained men. *J Appl Physiol*, 66(2): 704-711.

Mir, L. M., Bureau, M. F., Gehl, J., Rangara, R., Rouy, D., Caillaud, J. M., Delaere, P., Branellec, D., Schwartz, B., Scherman, D. 1999. High-efficiency gene transfer into skeletal muscle mediated by electric pulses. *Proc Natl Acad Sci U S A*, 96(8): 4262-4267.

Musi, N., Fujii, N., Hirshman, M. F., Ekberg, I., Froberg, S., Ljungqvist, O., Thorell, A., Goodyear, L. J. 2001. AMP-activated protein kinase (AMPK) is activated in muscle of subjects with type 2 diabetes during exercise. *Diabetes*, 50(5): 921-927.

Neubauer, N., Kulkarni, R. N. 2006. Molecular approaches to study control of glucose homeostasis. *ILAR J*, 47(3): 199-211.

Parker, P. J., Caudwell, F. B., Cohen, P. 1983. Glycogen synthase from rabbit skeletal muscle; effect of insulin on the state of phosphorylation of the seven phosphoserine residues in vivo. *Eur J Biochem*, 130(1): 227-234.

Pillay, T. S., Makgoba, M. W. 1991. Molecular mechanisms of insulin resistance. *S Afr Med J*, 79(10): 607-613.

Rak, A., Fedorov, R., Alexandrov, K., Albert, S., Goody, R. S., Gallwitz, D., Scheidig, A. J. 2000. Crystal structure of the GAP domain of Gyp1p: first insights into interaction with Ypt/Rab proteins. *EMBO J*, 19(19): 5105-5113.

Richardson, P. M., Zon, L. I. 1995. Molecular cloning of a cDNA with a novel domain present in the tre-2 oncogene and the yeast cell cycle regulators BUB2 and cdc16. *Oncogene*, 11(6): 1139-1148.

Richter, E. A., Garetto, L. P., Goodman, M. N., Ruderman, N. B. 1982. Muscle glucose metabolism following exercise in the rat: increased sensitivity to insulin. *J Clin Invest*, 69(4): 785-793.

Roach, P. J. 2002. Glycogen and its metabolism. *Curr Mol Med*, 2(2): 101-120.

Roach, W. G., Chavez, J. A., Miinea, C. P., Lienhard, G. E. 2007. Substrate specificity and effect on GLUT4 translocation of the Rab GTPase-activating protein Tbc1d1. *Biochem J*, 403(2): 353-358.

Roden, M., Price, T. B., Perseghin, G., Petersen, K. F., Rothman, D. L., Cline, G. W., Shulman, G. I. 1996. Mechanism of free fatty acid-induced insulin resistance in humans. *J Clin Invest*, 97(12): 2859-2865.

Rodriguez, I. R., Fliesler, S. J. 1988. A 42,000-Da protein in rabbit tissues and in a glycogen synthase preparation cross-reacts with antibodies to glycogenin. *Arch Biochem Biophys*, 260(2): 628-637.

Rubin, R. R., Fujimoto, W. Y., Marrero, D. G., Brenneman, T., Charleston, J. B., Edelstein, S. L., Fisher, E. B., Jordan, R., Knowler, W. C., Lichterman, L. C., Prince, M., Rowe, P. M. 2002. The Diabetes Prevention Program: recruitment methods and results. *Control Clin Trials*, 23(2): 157-171.

Ruderman, N. B., Saha, A. K., Vavvas, D., Witters, L. A. 1999. Malonyl-CoA, fuel sensing, and insulin resistance. *Am J Physiol*, 276(1 Pt 1): E1-E18.

Rune, A., Osler, M. E., Fritz, T., Zierath, J. R. 2009. Regulation of skeletal muscle sucrose, non-fermenting 1/AMP-activated protein kinase-related kinase (SNARK) by metabolic stress and diabetes. *Diabetologia*, 52(10): 2182-2189.

Saha, A. K., Schwarsin, A. J., Roduit, R., Masse, F., Kaushik, V., Tornheim, K., Prentki, M., Ruderman, N. B. 2000. Activation of malonyl-CoA decarboxylase in rat skeletal muscle by contraction and the AMP-activated protein kinase activator 5-aminoimidazole-4-carboxamide-1-beta -D-ribofuranoside. *J Biol Chem*, 275(32): 24279-24283.

Sakamoto, K., McCarthy, A., Smith, D., Green, K. A., Grahame Hardie, D., Ashworth, A., Alessi, D. R. 2005. Deficiency of LKB1 in skeletal muscle prevents AMPK activation and glucose uptake during contraction. *EMBO J*, 24(10): 1810-1820.

Schantz, P., Henriksson, J. 1983. Increases in myofibrillar ATPase intermediate human skeletal muscle fibers in response to endurance training. *Muscle Nerve*, 6(8): 553-556.

Scheffzek, K., Ahmadian, M. R., Wittinghofer, A. 1998. GTPase-activating proteins: helping hands to complement an active site. *Trends Biochem Sci*, 23(7): 257-262.

Schiaffino, S., Gorza, L., Sartore, S., Saggin, L., Ausoni, S., Vianello, M., Gundersen, K., Lomo, T. 1989. Three myosin heavy chain isoforms in type 2 skeletal muscle fibres. *J Muscle Res Cell Motil*, 10(3): 197-205.

Shen, S. W., Reaven, G. M., Farquhar, J. W. 1970. Comparison of impedance to insulin-mediated glucose uptake in normal subjects and in subjects with latent diabetes. *J Clin Invest*, 49(12): 2151-2160.

Smythe, C., Cohen, P. 1991. The discovery of glycogenin and the priming mechanism for glycogen biogenesis. *Eur J Biochem*, 200(3): 625-631.

Sogaard, P., Szekeres, F., Holmstrom, M., Larsson, D., Harlen, M., Garcia-Roves, P., Chibalin, A. V. 2009. Effects of fibre type and diffusion distance on mouse skeletal muscle glycogen content in vitro. *J Cell Biochem*, 107(6): 1189-1197.

Song, X. M., Fiedler, M., Galuska, D., Ryder, J. W., Fernstrom, M., Chibalin, A. V., Wallberg-Henriksson, H., Zierath, J. R. 2002. 5-Aminoimidazole-4-carboxamide ribonucleoside treatment improves glucose homeostasis in insulin-resistant diabetic (ob/ob) mice. *Diabetologia*, 45(1): 56-65.

Song, X. M., Ryder, J. W., Kawano, Y., Chibalin, A. V., Krook, A., Zierath, J. R. 1999. Muscle fiber type specificity in insulin signal transduction. *Am J Physiol*, 277(6 Pt 2): R1690-1696.

Spychala, J., Madrid-Marina, V., Fox, I. H. 1988. High Km soluble 5'-nucleotidase from human placenta. Properties and allosteric regulation by IMP and ATP. *J Biol Chem*, 263(35): 18759-18765.

Stone, S., Abkevich, V., Russell, D. L., Riley, R., Timms, K., Tran, T., Trem, D., Frank, D., Jammulapati, S., Neff, C. D., Iliev, D., Gress, R., He, G., Frech, G. C., Adams, T. D., Skolnick, M. H., Lanchbury, J. S., Gutin, A., Hunt, S. C., Shattuck, D. 2006. TBC1D1 is a candidate for a severe obesity gene and evidence for a gene/gene interaction in obesity predisposition. *Hum Mol Genet*, 15(18): 2709-2720.

Tanti, J. F., Grillo, S., Gremeaux, T., Coffer, P. J., Van Obberghen, E., Le Marchand-Brustel, Y. 1997. Potential role of protein kinase B in glucose transporter 4 translocation in adipocytes. *Endocrinology*, 138(5): 2005-2010.

Thorens, B. 2008. Glucose sensing and the pathogenesis of obesity and type 2 diabetes. *Int J Obes (Lond)*, 32 Suppl 6: S62-71.

Tkacs, N. C., Thompson, H. J. 2006. From bedside to bench and back again: research issues in animal models of human disease. *Biol Res Nurs*, 8(1): 78-88.

Van Breda, E., Keizer, H. A., Glatz, J. F., Geurten, P. 1990. Use of the intact mouse skeletal-muscle preparation for metabolic studies. Evaluation of the model. *Biochem J*, 267(1): 257-260.

Van Obberghen, E., Rossi, B., Kowalski, A., Gazzano, H., Ponzio, G. 1983. Receptor-mediated phosphorylation of the hepatic insulin receptor: evidence that the Mr 95,000 receptor subunit is its own kinase. *Proc Natl Acad Sci U S A*, 80(4): 945-949.

Wang, J., Obici, S., Morgan, K., Barzilai, N., Feng, Z., Rossetti, L. 2001. Overfeeding rapidly induces leptin and insulin resistance. *Diabetes*, 50(12): 2786-2791.

Wang, L. C., Kernell, D. 2001. Fibre type regionalisation in lower hindlimb muscles of rabbit, rat and mouse: a comparative study. *J Anat*, 199(Pt 6): 631-643.

White, R. A., Pasztor, L. M., Richardson, P. M., Zon, L. I. 2000. The gene encoding TBC1D1 with homology to the tre-2/USP6 oncogene, BUB2, and cdc16 maps to mouse chromosome 5 and human chromosome 4. *Cytogenet Cell Genet*, 89(3-4): 272-275.

Widmer, C. G., Morris-Wiman, J. A., Nekula, C. 2002. Spatial distribution of myosin heavy-chain isoforms in mouse masseter. *J Dent Res*, 81(1): 33-38.

Winder, W. W., Hardie, D. G. 1996. Inactivation of acetyl-CoA carboxylase and activation of AMP-activated protein kinase in muscle during exercise. *Am J Physiol*, 270(2 Pt 1): E299-304.

Young, M. E., Radda, G. K., Leighton, B. 1996. Activation of glycogen phosphorylase and glycogenolysis in rat skeletal muscle by AICAR--an activator of AMP-activated protein kinase. *FEBS Lett*, 382(1-2): 43-47.

Zeggini, E., Weedon, M. N., Lindgren, C. M., Frayling, T. M., Elliott, K. S., Lango, H., Timpson, N. J., Perry, J. R., Rayner, N. W., Freathy, R. M., Barrett, J. C., Shields, B., Morris, A. P., Ellard, S., Groves, C. J., Harries, L. W., Marchini, J. L., Owen, K. R., Knight, B., Cardon, L. R., Walker, M., Hitman, G. A., Morris, A. D., Doney, A. S., McCarthy, M. I., Hattersley, A. T. 2007. Replication of genome-wide association signals in UK samples reveals risk loci for type 2 diabetes. *Science*, 316(5829): 1336-1341.

Ziada, A. M., Hudlicka, O., Tyler, K. R., Wright, A. J. 1984. The effect of long-term vasodilatation on capillary growth and performance in rabbit heart and skeletal muscle. *Cardiovasc Res*, 18(12): 724-732.

Zierath, J. R., Wallberg-Henriksson, H. 1992. Exercise training in obese diabetic patients. Special considerations. *Sports Med*, 14(3): 171-189.